

NIED Seismic Moment Tensor Catalogue January – December, 1997

By

Eiichi Fukuyama*, Mizuho Ishida*, Shigeki Horiuchi*, Hiroshi Inoue*,
Sadaki Hori*, Shoji Sekiguchi*, Atsuki Kubo*, Hiroyuki Kawai[†],
Hiroshi Murakami[‡] and Ken'ichi Nonomura[†]

*National Research Institute for Earth Science and Disaster Prevention

[†]Sun Microsystems K.K.

[‡] Earthquake Observation Research Technology Center

Abstract

We have routinely estimated the moment tensors of earthquakes occurring in and around Japanese islands. This report compiles all the moment tensor solutions we have estimated in 1997. In these computations, we used the FREESIA/KIBAN broadband seismic network developed by NIED (National Research Institute for Earth Science and Disaster Prevention) and STA (Science and Technology Agency). We mainly used STS-1 broadband seismometer records. VSE311 strong motion velocity-meter was additionally used in cases when STS-1 waveforms were unavailable. Moment tensor estimation is triggered by the JMA (Japan Meteorological Agency) e-mail of emergent hypocenter location information. This catalogue includes most $M > 4.0$ earthquakes and some $M > 3.5$ earthquakes. However, due to either incomplete station distribution or the quality of available data, our catalog missed several earthquakes that had been detected by JMA.

Key words: Seismic moment tensor, Earthquake catalogue

1. Method

Below is a brief description of the method used here to determine seismic moment tensors and their centroid depths. Fukuyama et al. (1998) describes the method and it would be helpful to refer to this in more details. All the information concerning this catalogue is also displayed at the World Wide Web page¹. We already published the seismic moment tensor catalogue for 1998 (Fukuyama et al., 1999) and for 1999 (Fukuyama et al., 2000).

Moment tensor analysis is triggered by the JMA (Japan Meteorological Agency) emergency hypocenter report received by e-mail. The following information is used from the

¹<http://argent.geo.bosai.go.jp>

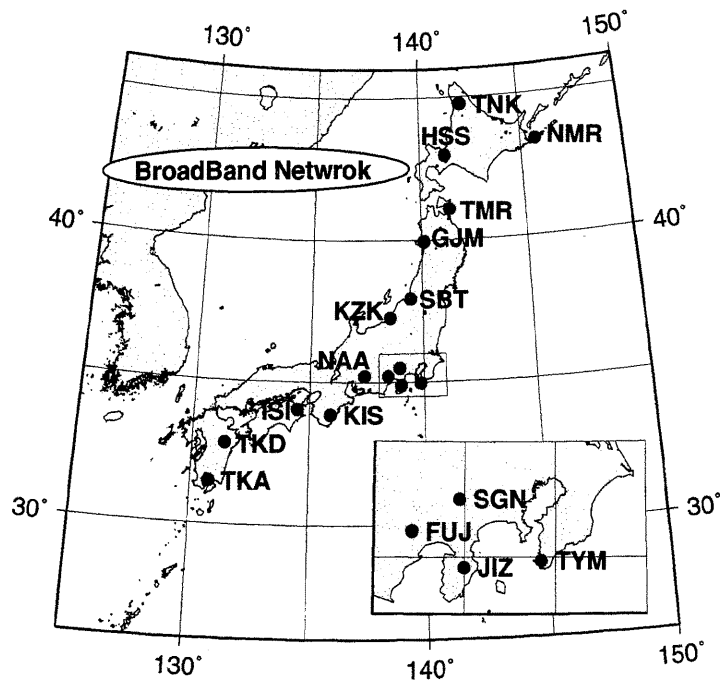


Fig. 1: Broadband station distribution used in the analysis.

report: origin time (in minutes), epicentral location (in 0.1 degree), depth (in 10km) and magnitude. This e-mail is dispatched for earthquakes with a maximum JMA scale intensity greater than 1 in the Kanto-Shinetsu-Chubu region (central part of Japan) and its surroundings. For other regions, the e-mail is dispatched only for earthquakes with a maximum intensity 3 or more. This information covers most $M > 3.5$ earthquakes. However, it sometimes misses off shore or deep $M > 3.5$ earthquakes, thus we used the information from the JWA (Japan Weather Association) World Wide Web page² as a supplement. We also took into account the relocated hypocenter information produced by JMA.

All the stations used in this analysis are shown in Fig. 1 and Table 1. Three stations at most are used for the moment tensor estimation. Filter coefficients and minimum epicentral distance are chosen according to the JMA magnitude (see Table 2). The JMA magnitude is used only for this purpose. The criterion for choosing stations is based on its epicentral distance. The closest three stations within the epicentral distance range are chosen as a first (automatic) trial. We then update it manually by examining station combinations, adjusting origin time offsets, or adjusting source depth. This is because if the waveforms are contaminated by long period noise, the solution is no more reliable. Manual operation is mainly employed to remove these noisy records. If the dataset is well examined, the moment tensor solution can be determined stably and uniquely by adjusting origin time offset and its source depth. In this catalogue, all solutions have been inspected and re-computed as final solutions.

Filtered displacement waveforms are used for the moment tensor inversion. The filter

²<http://tenki.or.jp/quake.html>

Table 1: Locations of stations used in the analysis.

Station Name	Station Code	Latitude ($^{\circ}N$)	Longitude ($^{\circ}E$)	Height (m)	Cooperative Organization	Funding Project
Fujigawa	FUJ	35.2267	138.4217	640	Tokyo U.	FREESIA
Gojyome	GJM	39.9517	140.1167	105	Tohoku U.	KIBAN
Sapporo	HSS	42.9647	141.2328	230	Hokkaido U.	FREESIA
Tokushima	ISI	34.0572	134.4580	27	Kyoto U.	FREESIA
Nakaizu	JIZ	34.9129	138.9972	263	—	FREESIA
Kiwa	KIS	33.8627	135.8933	70	Kyoto U.	FREESIA
Kashiwazaki	KZK	37.2951	138.5156	220	Tokyo U.	FREESIA
Asahi	NAA	35.2217	137.3650	200	Nagoya U.	FREESIA
Nemuro	NMR	43.3650	145.7430	20	Hokkaido U.	FREESIA
Shibata	SBT	37.9656	139.4538	160	Tohoku U.	KIBAN
Tsuru-Sugeno	SGN	35.5054	138.9475	800	—	FREESIA
Takakuma	TKA	31.5125	130.7853	535	Kagoshima U.	FREESIA
Takeda	TKD	32.8140	131.3900	751	Kyushu U.	FREESIA
Tomari	TMR	41.0990	141.3868	120	Hirosaki U.	KIBAN
Nakagawa	TNK	44.7757	142.0830	60	Hokkaido U.	FREESIA
Tateyama	TYM	34.9708	139.8481	30	Geogr. Surv. Jpn.	FREESIA

Table 2: Minimum epicentral distance, filter coefficients, and data length for initial magnitude reported by JMA

Magnitude range	Epicentral Dist. (km)	Frequency range (Hz)	Data length ($seconds$)
3.5 <M <5.0	>50	0.02 – 0.05	120
5.0 <M <6.5	>100	0.01 – 0.05	120
6.5 <M <7.5	>300	0.01 – 0.05	150
7.5 <M	>600	0.005 – 0.02	180

coefficients vary according to JMA magnitude (Table 2). 1 Hz sampling displacement data produced from the original 20Hz data stream (VBB components) are used in order to reduce the latency caused by packeting during the transmission from each station.

The moment tensor estimation consists of two steps, an automatic process and a manual one with human inspections. In the automatic stage, by using JMA e-mail, three stations are chosen automatically to prepare the waveform dataset. Using these waveforms, a moment tensor inversion is conducted with several trial depths within $\pm 30km$ from the JMA hypocenter depth. Assumed depth points are shown in Table 3. In the manual determination stage, the combination of stations, optimum zero offset and depth have been examined by the operator in a Monte Carlo manner. At this point, the error function is set to variance

Table 3: Assumed source depths in km used in the analysis.

5	8	11	14	17	20	23	26	29	32	35	38	41	44	47	50	53	56	59	62	65	68
71	74	77	80	83	86	89	92	95	98	101	104	107	110	113	116	119	122				
125	130	135	140	145	150	155	160	165	170	175	180	185	190	195	200						
210	220	230	240	250	260	270	280	290	300	320	340	360	380	400							

Table 4: Velocity structure for Green's functions.

Depth (km)	Thickness (km)	P Velocity (km/s)	S Velocity (km/s)	Density (kg/m ³)	Q_P	Q_S
0	3	5.50	3.14	2300	600	300
3	15	6.00	3.55	2400	600	300
18	15	6.70	3.83	2800	600	300
33	67	7.80	4.46	3200	600	300
100	125	8.00	4.57	3300	600	300
225	100	8.40	4.80	3400	600	300
325	100	8.60	4.91	3500	600	300
425	–	9.30	5.31	3700	600	300

reduction (*VarRed*) defined as follows:

$$VarRed = 100 \times \sum_i w_i \int \left(1 - \frac{(s_i(t) - o_i(t))^2}{|s_i(t)||o_i(t)|} \right) dt \quad [\%] \quad (1)$$

where $s_i(t)$ and $o_i(t)$ are synthetic and observed waveforms respectively. w_i is a weighting function proportional to the hypocentral distance.

The velocity structure used for Green's function is shown in Table 4. This structure is constructed by referring to Ukawa et al. (1984) for the shallower part and Fukao (1977) for the deeper part. Green's function is computed by using the discrete wavenumber method developed by Saikia (1994). The program named *tdmt_inv* is used for the moment tensor estimation which is developed by Pasyanos et al. (1996). *tdmt_sched.pl* is a Perl script developed here and used in the routine process. *tdmt_sched.pl* controls the automatic procedure. *tdmt_manual.pl* then supports the human inspection of the automatic moment tensor solution by referring to the automatic solution. In this inversion, since the time offset is shifted either automatically or manually, the centroid location is not estimated. This offset adjustment corrects both velocity structure misfit and the misfit between hypocenter and centroid location. As shown in Fukuyama et al. (1998), the shape of Green's function does not change for slight epicentral distance change, so that the above procedure works.

2. Results

The results are shown in Table 5, Figs. 2 and 3. In Table 5, origin times, latitudes, longitudes and region names are provided by JMA e-mail. Other parameters such as D (depth), Mw (moment magnitude) etc., are determined by this analysis. VarRed represents variance reduction, shown as percentages. (Str1, Dip1, Rak1) and (Str2, Dip2, Rak2) are two fault planes. Str, Dip, and Rak indicate strike, dip and rake angles, respectively. M_{xx} , M_{xy} , M_{xz} , M_{yy} , M_{yz} , and M_{zz} are the moment tensor components normalized by M_o (total scalar moment). In Fig. 2, moment tensors with the best fit double couples are shown in addition to their epicentral locations. The numerals appearing above each moment tensor represent the event ID shown in Table 5. In Fig 3, moment tensors are shown with lower hemisphere projection. P- and T- axes are also shown. Superscripted numerals again indicate event ID.

3. Conclusion

We have estimated 315 seismic moment tensors and their centroid depths by using FREESIA/KIBAN broadband waveforms.

Acknowledgments

The FREESIA broadband seismic network is supported by the NIED project entitled ‘Fundamental Research on Earthquakes and the Earth’s Interior Anomaly’ under the cooperation of Hokkaido University, Tokyo University, Nagoya University, Kyoto University, Kyushu University, Kagoshima University, and the Geographical Survey of Japan. The KIBAN broadband seismic network is supported by the Science and Technology Agency under the cooperation of the Headquarters for Earthquake Research Promotion. Finally we would appreciate Professor Douglas S. Dreger for providing us with the core code for moment tensor analysis as well as for his devoted assistance.

References

- 1) Fukao, Y. (1977): Upper mantle P structure on the ocean side of the Japan–Kurile Arc, *Geophys. J. Roy. astr. Soc.*, **50**, 621-642.
- 2) Fukuyama, E., M. Ishida, D. S. Dreger and H. Kawai (1998): Automated seismic moment tensor determination by using on-line broadband seismic waveforms, *Zisin*, **51**, 149-156 (in Japanese with English abstract).
- 3) Fukuyama, E., M. Ishida, S. Horiuchi, H. Inoue, S. Hori, S. Sekiguchi, H. Kawai, and H. Murakami (1999): NIED seismic moment tensor catalogue January - December, 1998, *Technical Note of the National Research Institute for Earth Science and Disaster Prevention*, **193**, 1-35.
- 4) Fukuyama, E., M. Ishida, S. Horiuchi, H. Inoue, S. Hori, S. Sekiguchi, H. Kawai, H. Murakami, S. Yamamoto, K. Nonomura, and A. Goto (2000): NIED seismic moment

tensor catalogue January - December, 1999, *Technical Note of the National Research Institute for Earth Science and Disaster Prevention*, **199**, 1-56.

- 5) Pasyanos, M. E., D. S. Dreger and B. Romanowicz (1996): Toward real-time estimation of regional moment tensors, *Bull. Seismol. Soc. Am.*, **86**, 1255-1269.
- 6) Saikia, C. K. (1994): Modified frequency-wavenumber algorithm for regional seismograms using Filon's quadrature: modelling of Lg wave in eastern North America, *Geophys. J. Int.*, **118**, 142-158.
- 7) Ukawa, M., M. Ishida, S. Matsumura, and K. Kasahara (1984): Hypocenter determination method of the Kanto-Tokai observational network for microearthquakes, *Research Notes of the National Research Center for Disaster Prevention*, **53**, 1-88 (in Japanese with English abstract).

NIED 地震モーメントテンソルカタログ

1997年1月-12月

福山英一*・石田瑞穂*・堀内茂木*・井上公*・堀貞喜*・関口渉次*・
久保篤規*・川井啓廉†・村上寛史‡・野々村健一†

要旨

我々は、日本及びその周辺で発生する地震のモーメントテンソルを定常的に決めている。このレポートは、1997年に決められたすべての地震のモーメントテンソル解をコンパイルしたものである。防災科学技術研究所及び科学技術庁により整備された広帯域地震観測網のデータを用いて計算を行った。解析には主に STS-1 型広帯域地震計の波形を用いたが、利用できない場合は、VSE311 型速度型強震計を用いた。気象庁から発信される緊急震源情報を含んだ電子メールにより解析を開始させた。本カタログは、ほとんどのマグニチュード 4 以上の地震といくつかのマグニチュード 3.5 以上の地震をカバーしている。しかしながら、観測点分布の偏りや、波形データのノイズ状況により、気象庁により検知された地震のいくつかは解が決まらず、カタログからは洩れている。

キーワード：モーメントテンソル, 地震カタログ

*防災科学技術研究所

†サン・マイクロシステムズ株式会社

‡有限会社 地震観測技術センター

Table 5: Estimated moment tensors (continued).

Table with 28 columns: No., Origin Time (UT), Lat (N), Lon (E), D (km), Mw, Ms (Nm), Var Red, Region name, Stri, Dip1, Rak1, Str2, Dip2, Rak2, Mxx, Mxy, Mxz, Myy, Myz, Mzz, used Stations. The table lists 314 seismic events with their respective parameters and station identifiers.

Table 5: Estimated moment tensors (continued).

No.	Origin Time(UT)	Lat(N)	Lon(E)	D(km)	Mw	M ₀ (Nm)	VarRec	Region name	Str1	Dip1	Rak1	Str2	Dip2	Rak2	Mxx	Myy	Mzz	Mxy	Mxz	Myz	Mzz	used Stations
282	1997/11/23/03:30	40.0	138.8	8	3.3	2.2e17	51.46	W off Akita pref	12	51	87	197	39	94	-0.0102	0.2524	0.0130	-0.9390	0.0130	-0.2261	0.9491	TMR KZK
283	1997/11/23/08:39	40.0	138.2	11	3.8	5.0e14	74.30	W off Akita pref	35	74	124	150	37	27	0.3262	0.0519	0.6008	-0.7645	-0.4443	0.4383	TMR KZK	
284	1997/11/28/04:36	32.4	147.2	53	3.8	3.0e14	86.64	NE off Iwate pref	123	73	96	178	17	66	-0.0096	0.0956	0.3571	-0.3584	-0.7398	0.5680	TMR GJM HSS	
285	1997/11/28/04:36	32.4	147.2	29	3.3	6.0e15	76.64	far S off Tokai District	110	82	-167	278	27	17	-0.0595	0.1919	-0.3465	0.6150	0.0611	-0.0555	KIS	
286	1997/12/01/18:17	40.0	139.0	56	4.7	9.2e16	88.79	SW Ibaraki pref	41	67	170	278	143	143	-0.0521	0.2174	0.3430	-0.6912	-0.6648	0.5309	FUJ KZK	
287	1997/12/01/18:17	40.0	138.9	8	4.7	9.2e16	88.79	SE off Kii Akita pref	50	88	171	116	19	175	-0.1894	0.3833	-0.3325	0.1798	-0.3357	0.6795	GJM TMR HSS	
288	1997/12/02/08:18	34.0	136.4	400	4.6	8.5e15	58.70	W off Akita pref	205	88	86	39	34	93	-0.3248	0.3833	-0.3325	-0.5892	0.3983	0.0129	NAA FUJ SGN HSS	
289	1997/12/05/23:57	34.3	139.1	11	3.9	9.2e14	66.08	W off Akita pref	310	86	149	42	50	4	-0.3668	0.1137	-0.3463	0.8197	-0.3683	0.9069	GJM TMR HSS	
290	1997/12/06/06:40	35.7	140.1	32	4.7	1.31e16	89.42	near Niijima island	269	68	-155	10	64	-155	0.2686	-0.7910	0.3864	0.0178	-0.3852	0.0163	JIZ FUJ SGN HSS	
291	1997/12/06/23:02	35.7	140.1	32	4.2	1.95e15	87.33	northern Chiba pref	16	69	-133	265	46	-29	0.3890	-0.6081	0.1615	0.0821	0.6539	-0.4711	SGN FUJ KZK HSS	
292	1997/12/07/03:50	37.7	141.8	83	5.4	1.25e17	89.18	E off Fukushima pref	192	50	-96	21	40	-83	0.1048	-0.2628	-0.0335	0.8947	-0.1801	-0.9995	SGN FUJ KZK HSS	
293	1997/12/08/06:49	37.7	141.1	65	3.7	4.67e14	51.38	E off Fukushima pref	131	88	154	222	64	25	-0.8470	0.1388	0.2601	0.9174	0.3860	-0.0704	KZK SGN FUJ HSS	
294	1997/12/09/19:21	36.5	141.1	44	4.3	3.51e15	88.70	E off Ibaraki pref	88	74	127	198	39	25	-0.4052	0.6088	0.6768	-0.0105	0.0754	0.4157	SGN KZK FUJ HSS	
295	1997/12/13/06:45	39.6	142.4	71	4.6	8.77e15	85.23	E off Iwate pref	254	65	-102	101	28	-65	0.6386	0.0575	0.5579	0.2657	-0.3688	-0.9043	TMR GJM SBT HSS	
296	1997/12/16/11:34	40.5	140.0	165	4.3	3.39e15	83.86	western Amori pref	148	66	-28	250	65	153	0.8333	0.5211	0.1435	-0.4704	-0.4327	-0.3629	GJM SBT HSS	
297	1997/12/19/13:07	36.3	136.2	8	4.3	3.22e15	86.56	central Fukui pref	202	58	71	55	36	118	-0.1885	0.6407	-0.0845	-0.5624	0.4069	0.7509	NAA SGN KIS HSS	
298	1997/12/21/21:03	43.1	146.4	44	5.1	5.46e16	70.49	off Nemuro peninsula	326	46	-81	134	45	-99	0.4068	0.4977	-0.0821	0.5816	0.0757	-0.9884	TNK GJM HSS	
299	1997/12/22/16:31	40.2	142.5	47	5.3	1.19e17	91.30	NE off Iwate pref	222	70	94	191	20	81	-0.0980	0.1479	0.3023	-0.5774	-0.6953	0.6754	TMR GJM HSS	
300	1997/12/22/19:08	43.0	143.5	113	5.1	4.62e16	77.23	Tokachi region	290	87	-62	25	28	-175	0.3863	-0.3293	0.8247	-0.3117	-0.2948	-0.0746	TMR GJM HSS	
301	1997/12/23/06:18	36.2	140.9	38	4.3	3.32e15	89.43	E off Ibaraki pref	340	77	56	232	36	158	0.3119	0.2909	-0.3763	-0.6624	0.6610	0.3505	SGN KZK FUJ HSS	
302	1997/12/23/11:08	41.0	139.3	17	3.9	7.38e14	91.48	W off Amori pref	2	89	-121	270	31	-2	0.0377	-0.5207	-0.0078	-0.0085	0.8523	-0.3133	GJM TMR HSS	
303	1997/12/24/08:08	43.6	147.3	35	3.8	5.98e14	71.64	E off Hokkaido	114	73	134	220	47	24	-0.8766	0.2006	0.4734	0.4397	0.3416	0.4159	NAA TKD HSS	
304	1997/12/24/11:30	31.1	127.9	14	4.4	4.96e15	88.62	east China sea region	227	87	-131	133	41	-5	0.7081	-0.0245	0.5364	-0.6162	-0.5176	-0.2019	TMR TKD HSS	
305	1997/12/24/12:31	34.8	140.1	50	3.5	1.72e14	74.06	SE off Boso peninsula	27	82	49	287	41	168	-0.5691	0.4428	0.2047	0.3659	-0.7152	0.9019	SGN FUJ HSS	
306	1997/12/24/15:17	31.8	140.1	11	4.0	9.89e14	96.77	NW Kagoshima pref	290	80	15	197	75	169	0.6618	-0.7548	-0.3193	0.5764	0.1033	0.0146	TKD ISI KIS HSS	
307	1997/12/26/04:26	33.2	132.2	41	3.7	4.08e14	85.77	Bungo channel	63	72	28	324	64	160	-0.9056	-0.3829	0.2175	0.6290	-0.4016	0.2768	TKD ISI KIS HSS	
308	1997/12/26/17:29	40.6	144.1	11	4.3	3.18e15	76.24	far E off Sanriku	30	56	105	185	37	69	0.0186	0.3282	0.2797	-0.8812	-0.2441	0.8628	TMR GJM NAA HSS	
309	1997/12/27/01:08	34.1	135.1	8	3.8	5.03e14	91.73	NW Wakayama pref	338	52	64	196	44	119	0.1424	-0.0580	-0.3149	-1.0038	-0.1197	0.8614	ISI KIS NAA HSS	
310	1997/12/28/05:13	40.6	144.0	8	4.6	1.00e16	51.93	far E off Sanriku	35	56	101	197	36	75	-0.1826	0.3559	0.3011	-0.7478	-0.2328	0.9304	TMR GJM HSS	
311	1997/12/28/23:31	36.1	138.6	190	4.0	1.06e15	89.86	eastern Nagano pref	9	88	-48	100	42	-177	-0.1599	0.6359	-0.2034	0.1880	0.7235	-0.0280	SGN FUJ NAA HSS	
312	1997/12/29/06:13	42.8	145.5	53	4.0	1.02e15	81.09	off Nemuro peninsula	241	85	-161	149	71	-5	0.6273	0.4820	0.2369	-0.7925	-0.2359	-0.0348	HSS FUJ NAA HSS	
313	1997/12/29/16:11	35.7	140.8	47	4.1	1.40e15	89.99	near Choshi city	345	66	92	160	24	85	-0.0259	-0.3293	-0.1679	-0.6939	-0.6503	0.7198	SGN FUJ KZK HSS	
314	1997/12/31/01:16	43.3	146.7	98	5.4	1.49e17	80.18	off Nemuro peninsula	283	83	138	19	48	10	-0.4739	0.6299	-0.6134	0.3114	-0.2389	0.1625	NMR	
315	1997/12/31/22:27	34.1	135.2	5	3.5	2.32e14	66.07	NW Wakayama pref	14	57	114	155	40	58	0.1479	-0.1006	0.2856	-0.9731	-0.2944	0.8253	ISI KIS NAA HSS	

Jan, 1,1997 - Jan,31,1997 (UT)

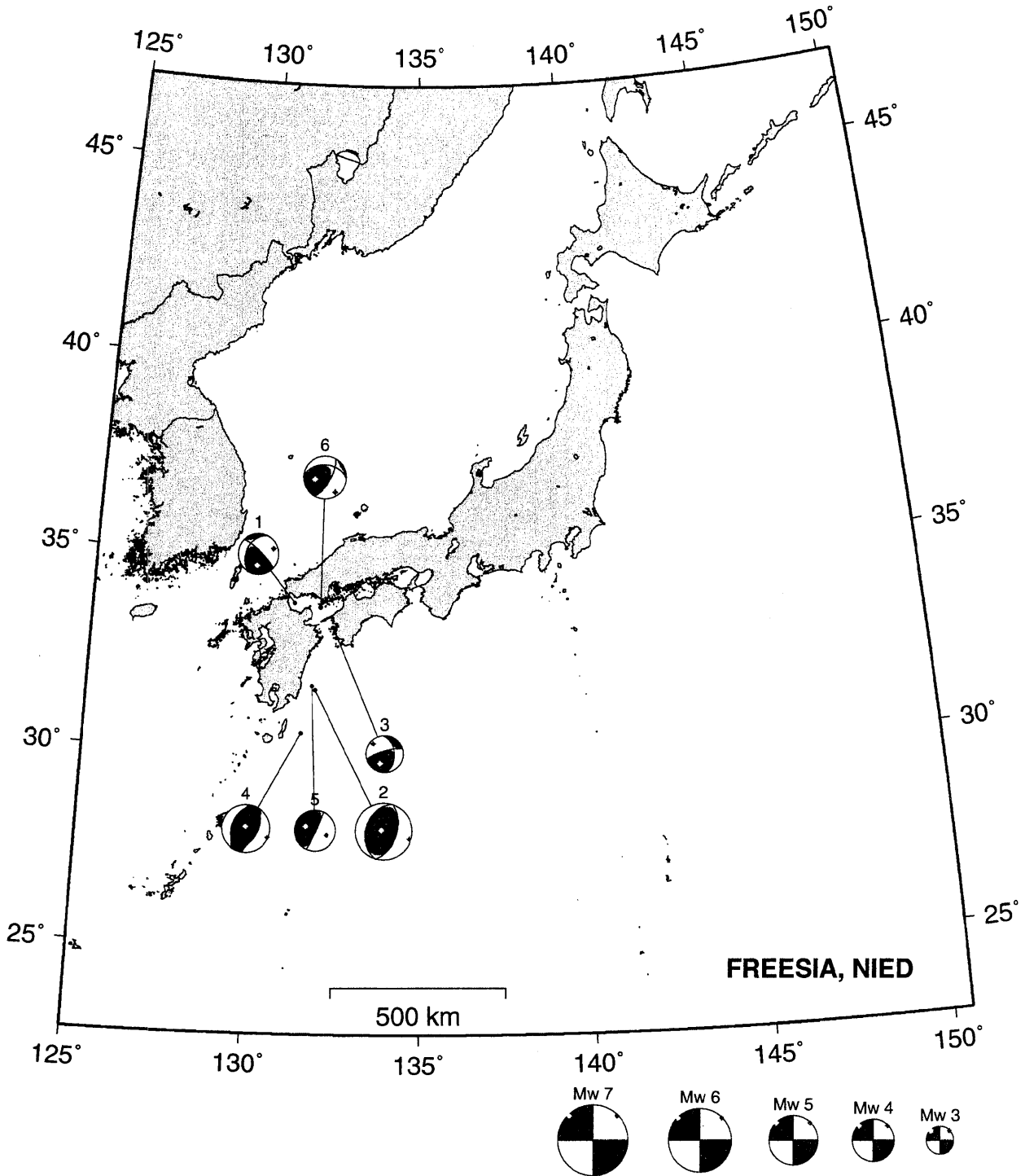


Fig. 2: Estimated moment tensors plotted with epicentral locations.

Feb, 1, 1997 - Feb, 28, 1997 (UT)

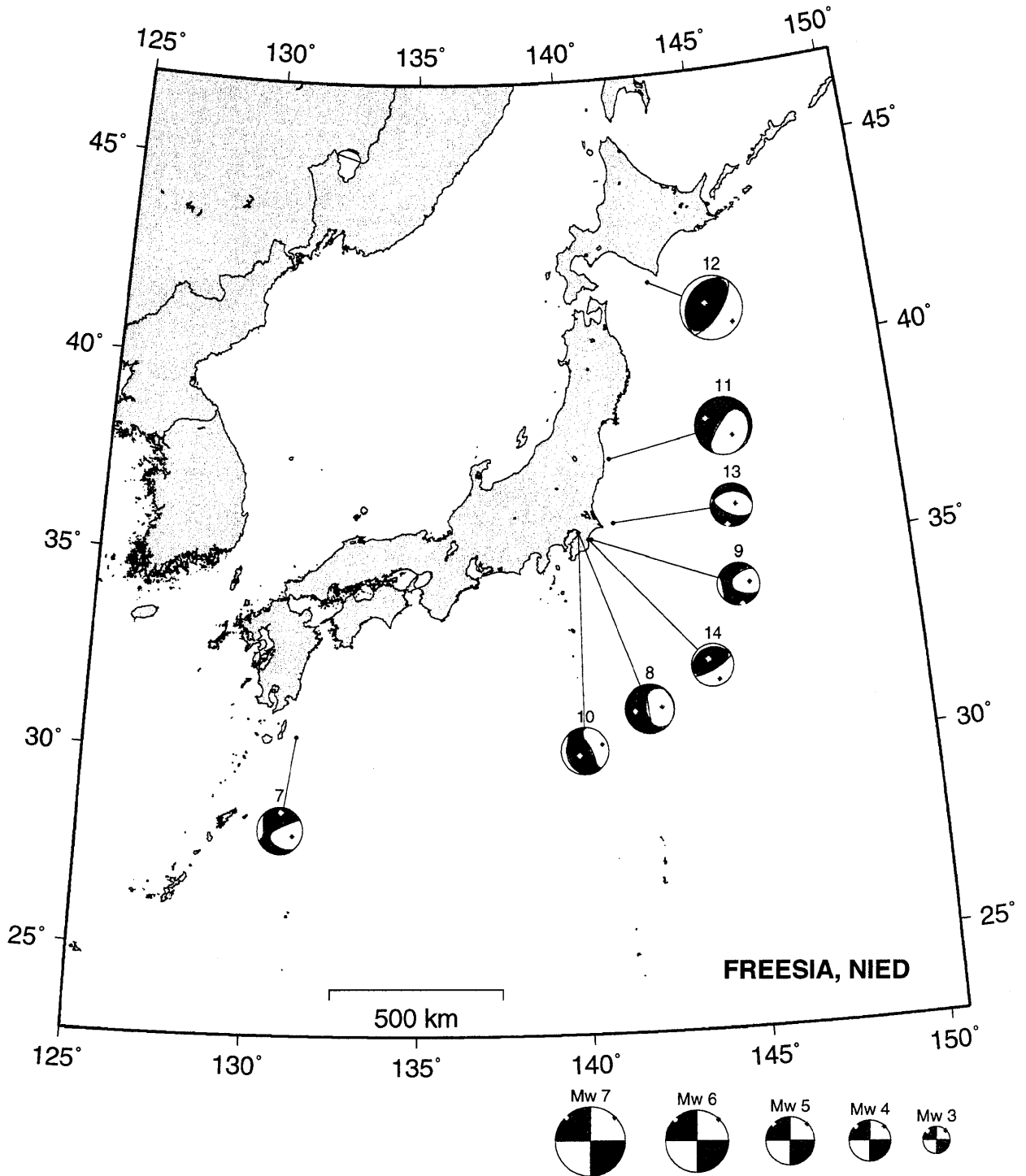


Fig. 2: Estimated moment tensors plotted with epicentral locations (continued).

Mar, 1, 1997 - Mar, 31, 1997 (UT)

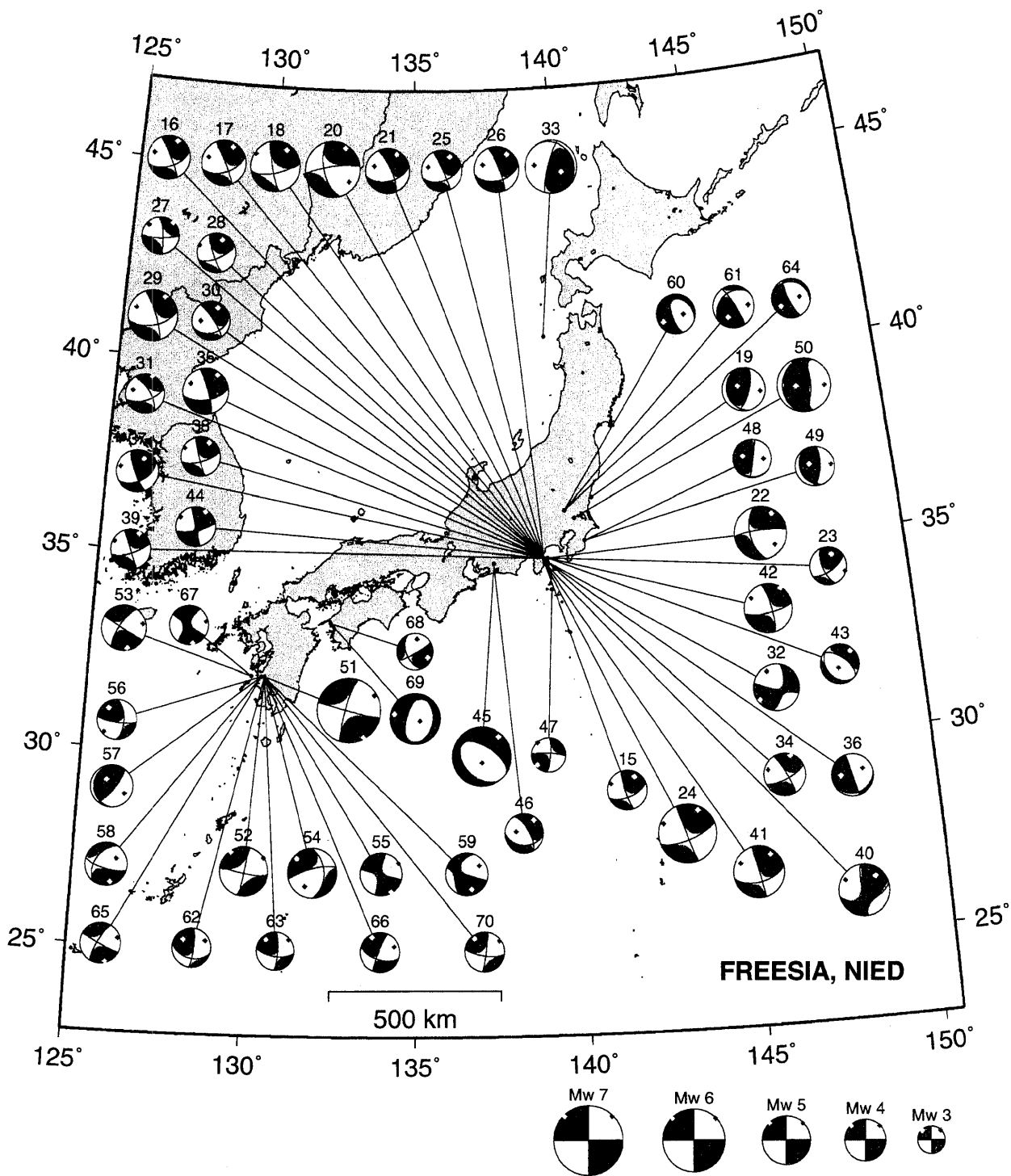


Fig. 2: Estimated moment tensors plotted with epicentral locations (continued).

Apr, 1, 1997 - Apr, 30, 1997 (UT)

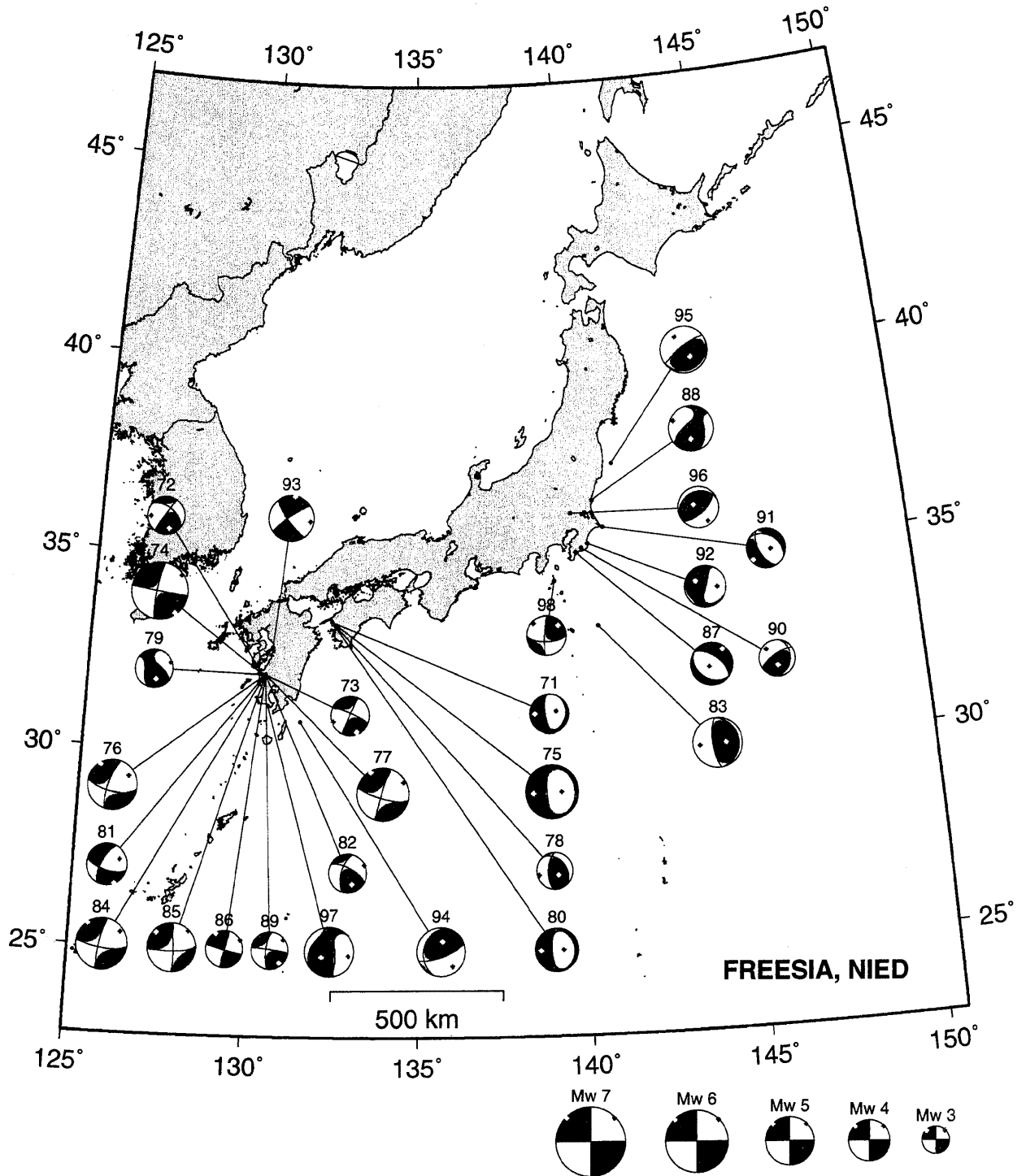


Fig. 2: Estimated moment tensors plotted with epicentral locations (continued).

May, 1, 1997 - May, 31, 1997 (UT)

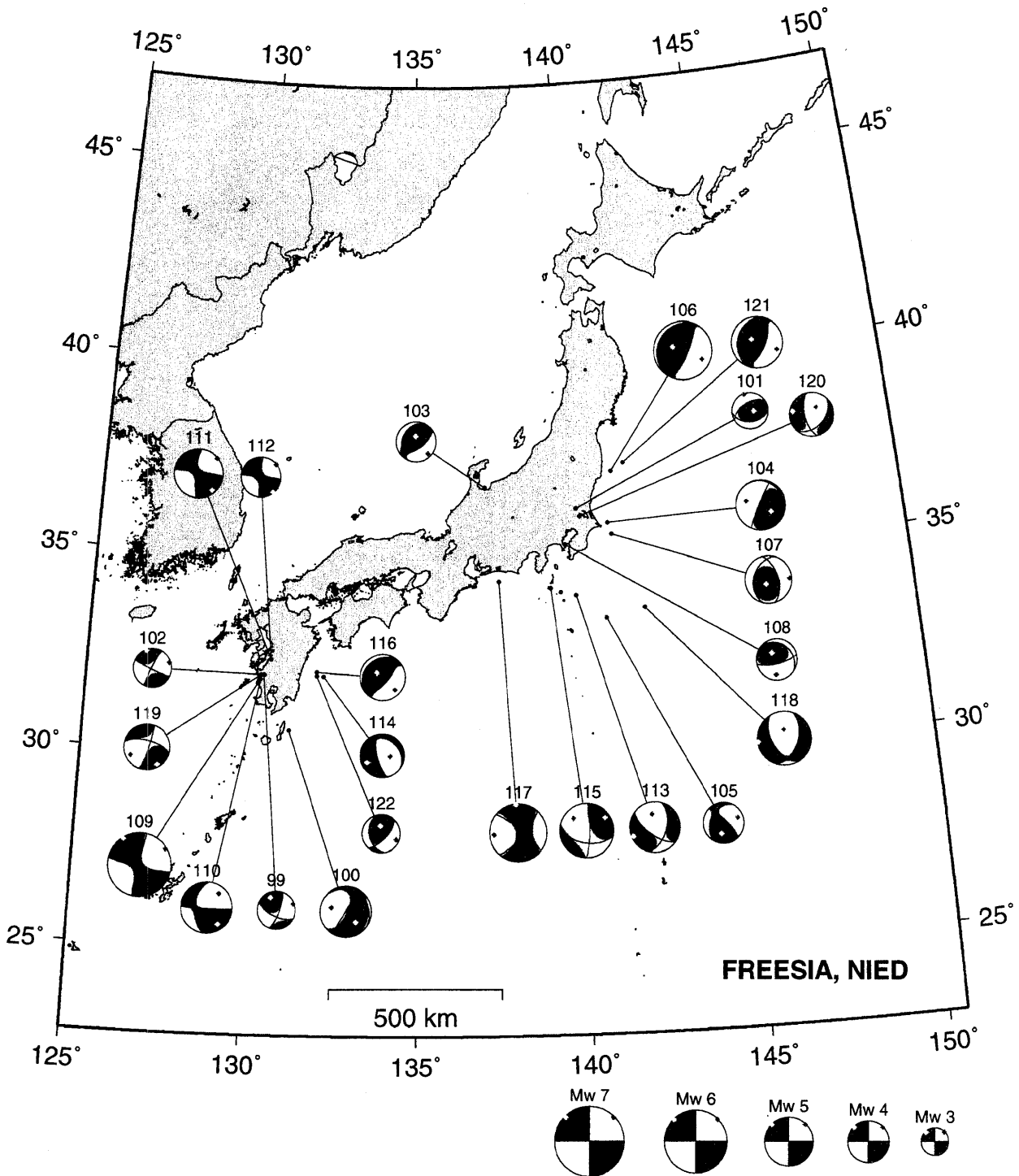


Fig. 2: Estimated moment tensors plotted with epicentral locations (continued).

Jun, 1, 1997 - Jun, 30, 1997 (UT)

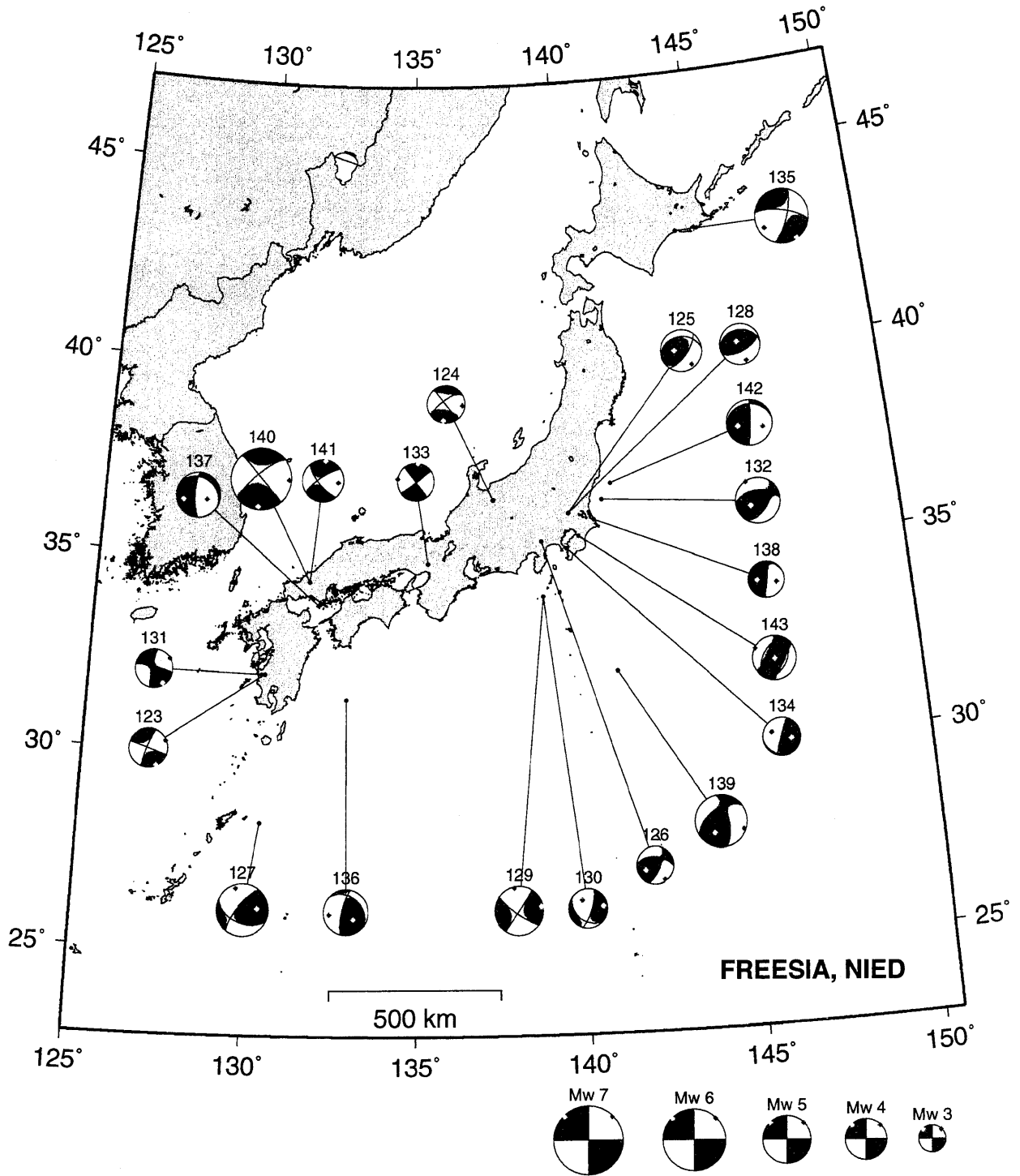


Fig. 2: Estimated moment tensors plotted with epicentral locations (continued).

Jul, 1, 1997 - Jul, 31, 1997 (UT)

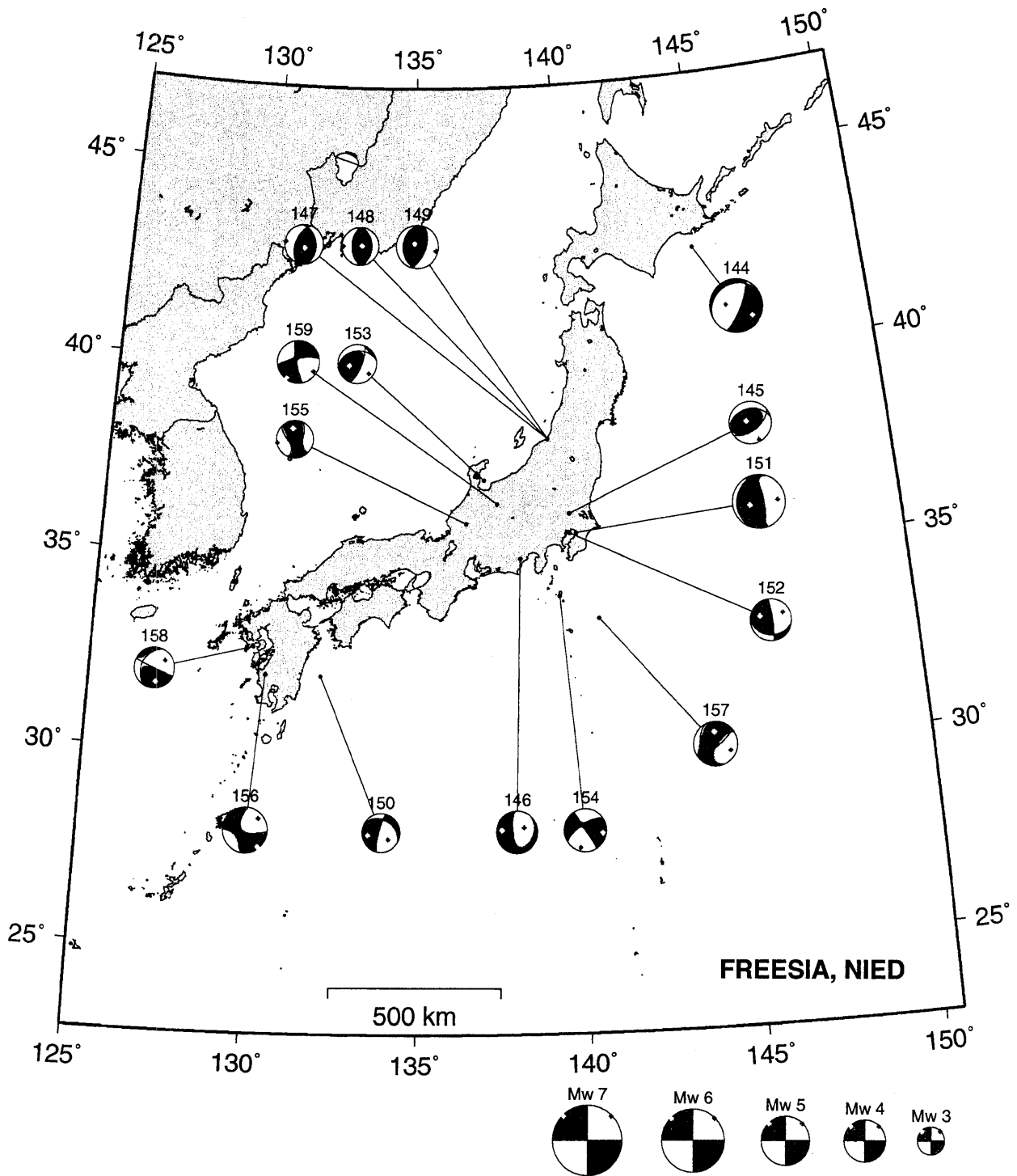


Fig. 2: Estimated moment tensors plotted with epicentral locations (continued).

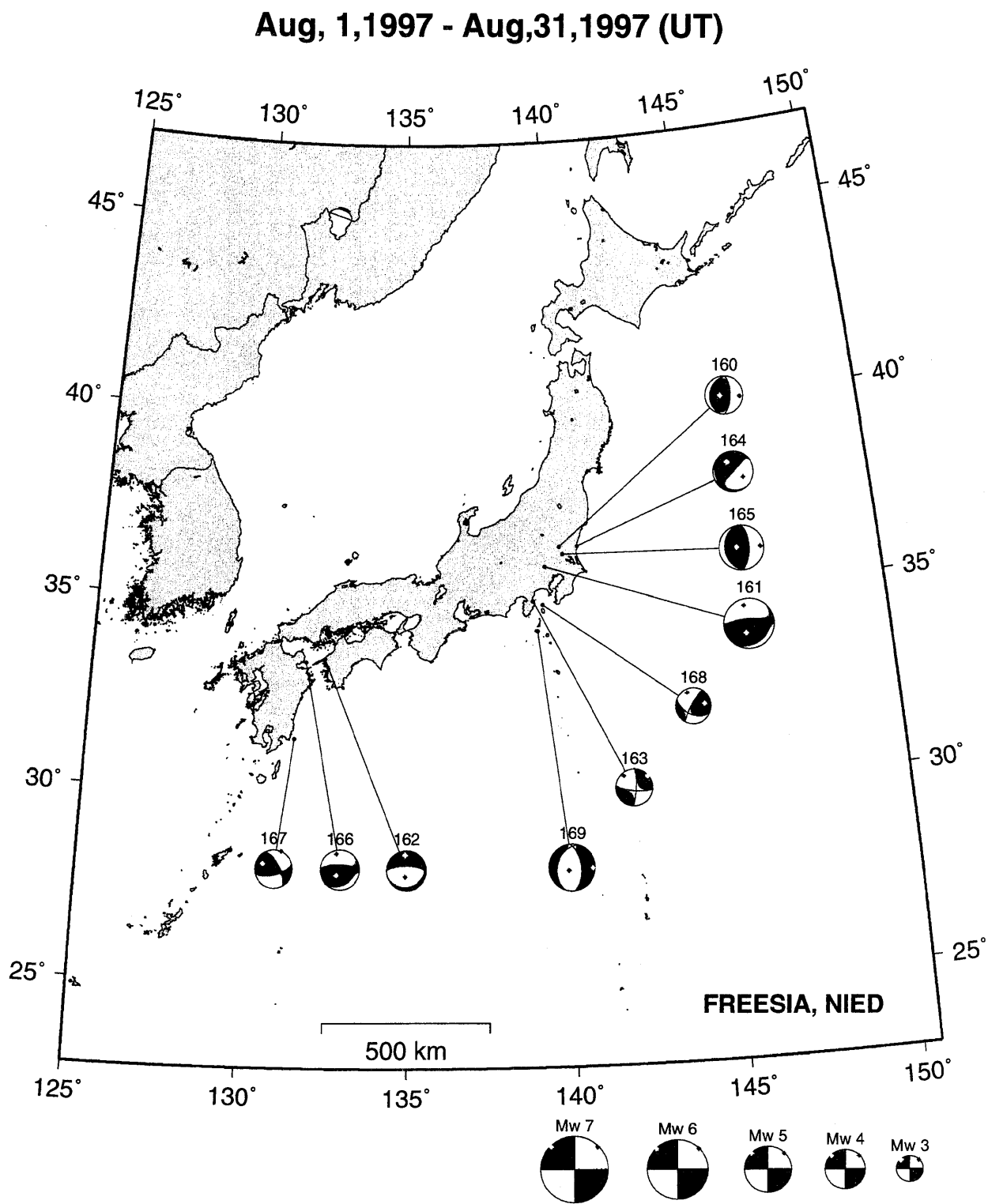


Fig. 2: Estimated moment tensors plotted with epicentral locations (continued).

Sep, 1, 1997 - Sep, 30, 1997 (UT)

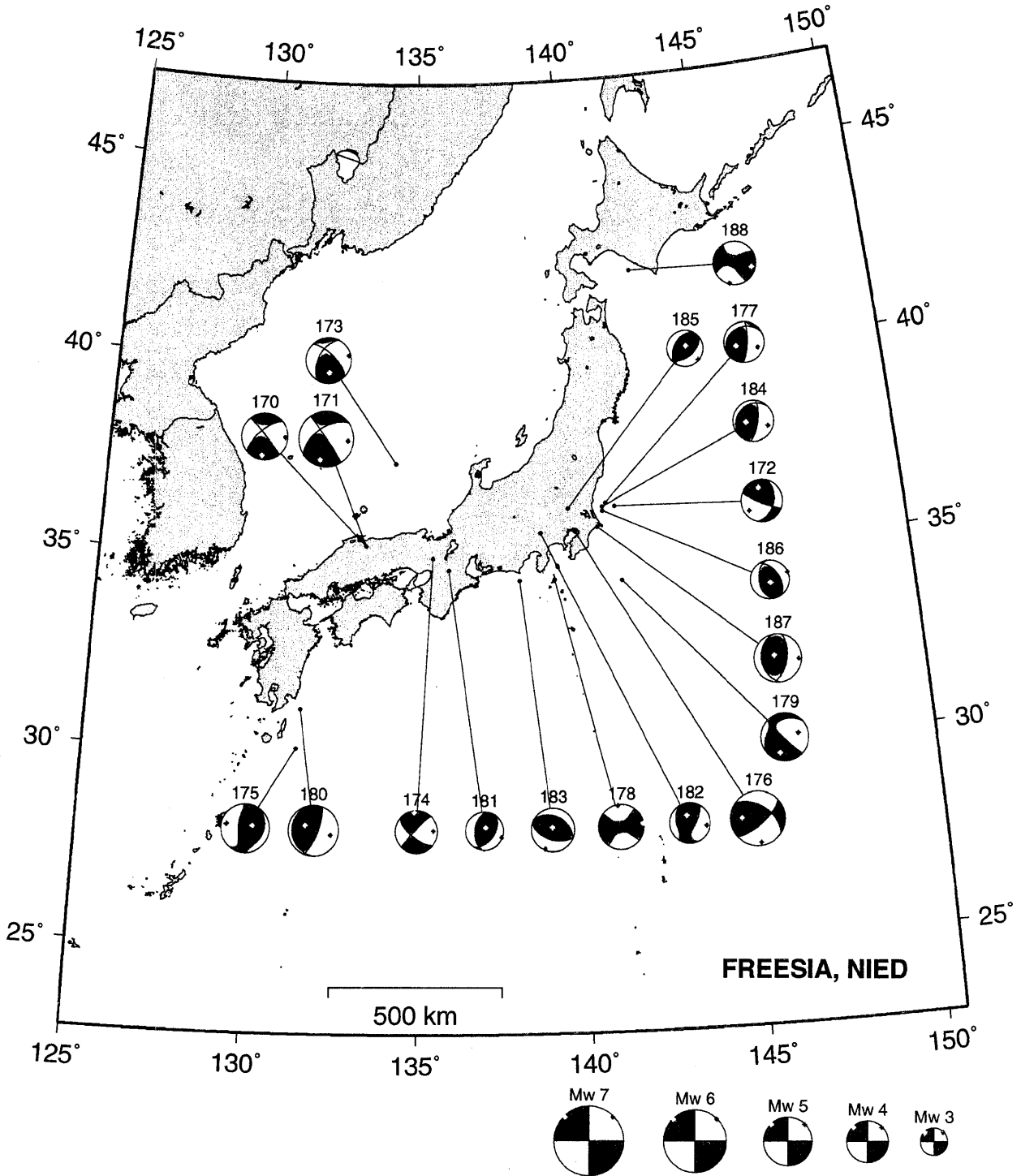


Fig. 2: Estimated moment tensors plotted with epicentral locations (continued).

Oct, 1, 1997 - Oct, 31, 1997 (UT)

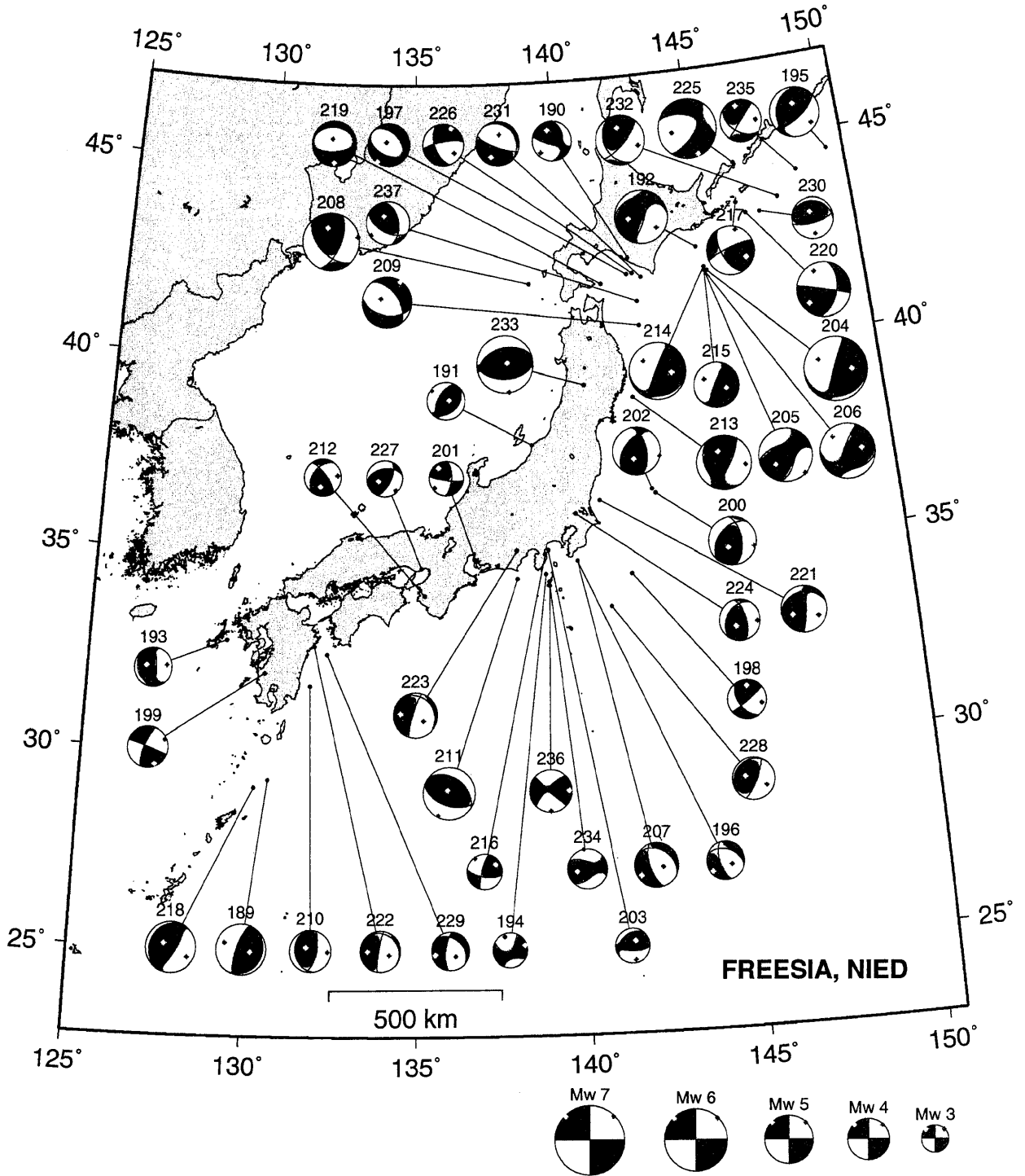


Fig. 2: Estimated moment tensors plotted with epicentral locations (continued).

Nov, 1, 1997 - Nov, 30, 1997 (UT)

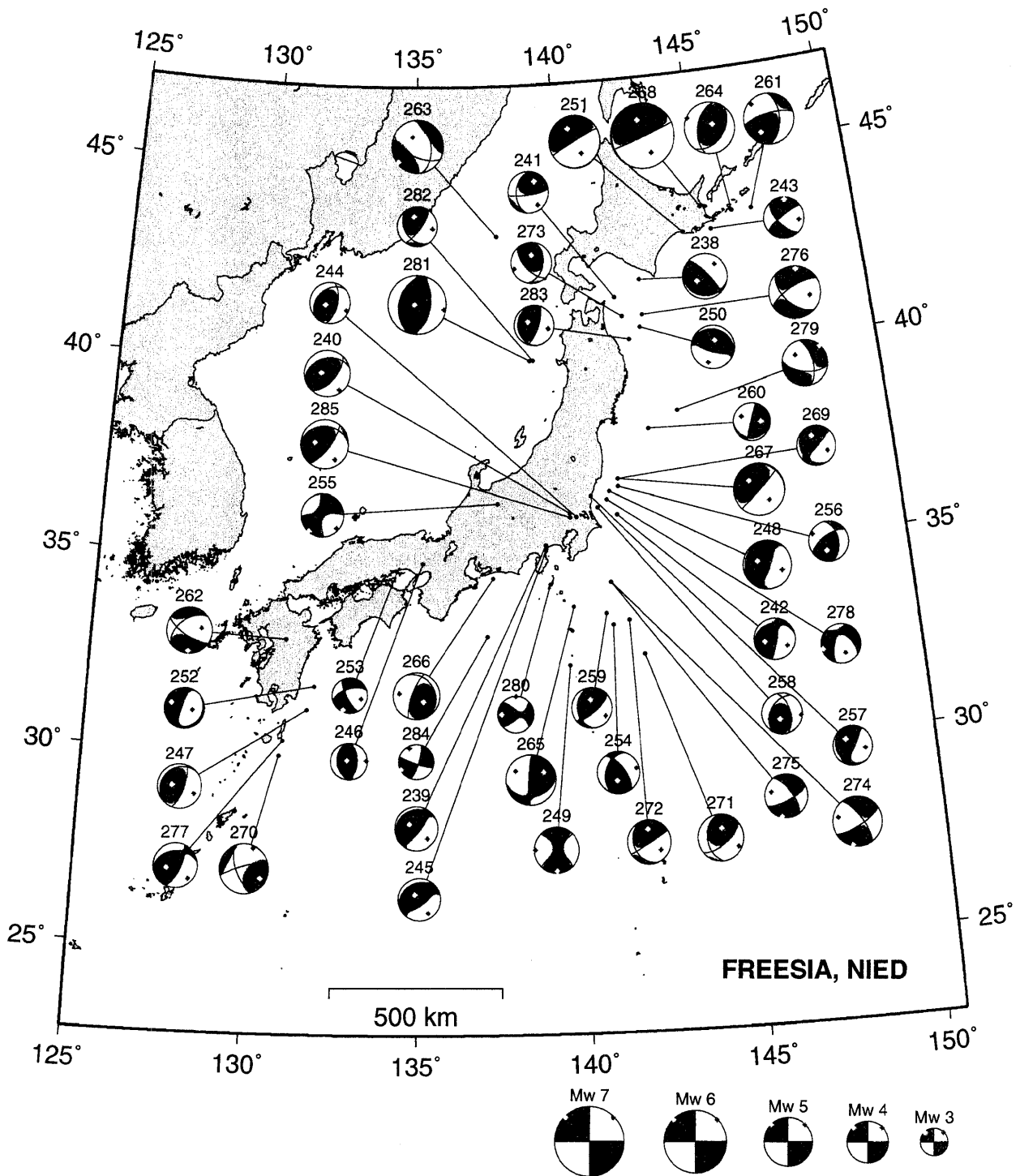


Fig. 2: Estimated moment tensors plotted with epicentral locations (continued).

Dec, 1,1997 - Dec,31,1997 (UT)

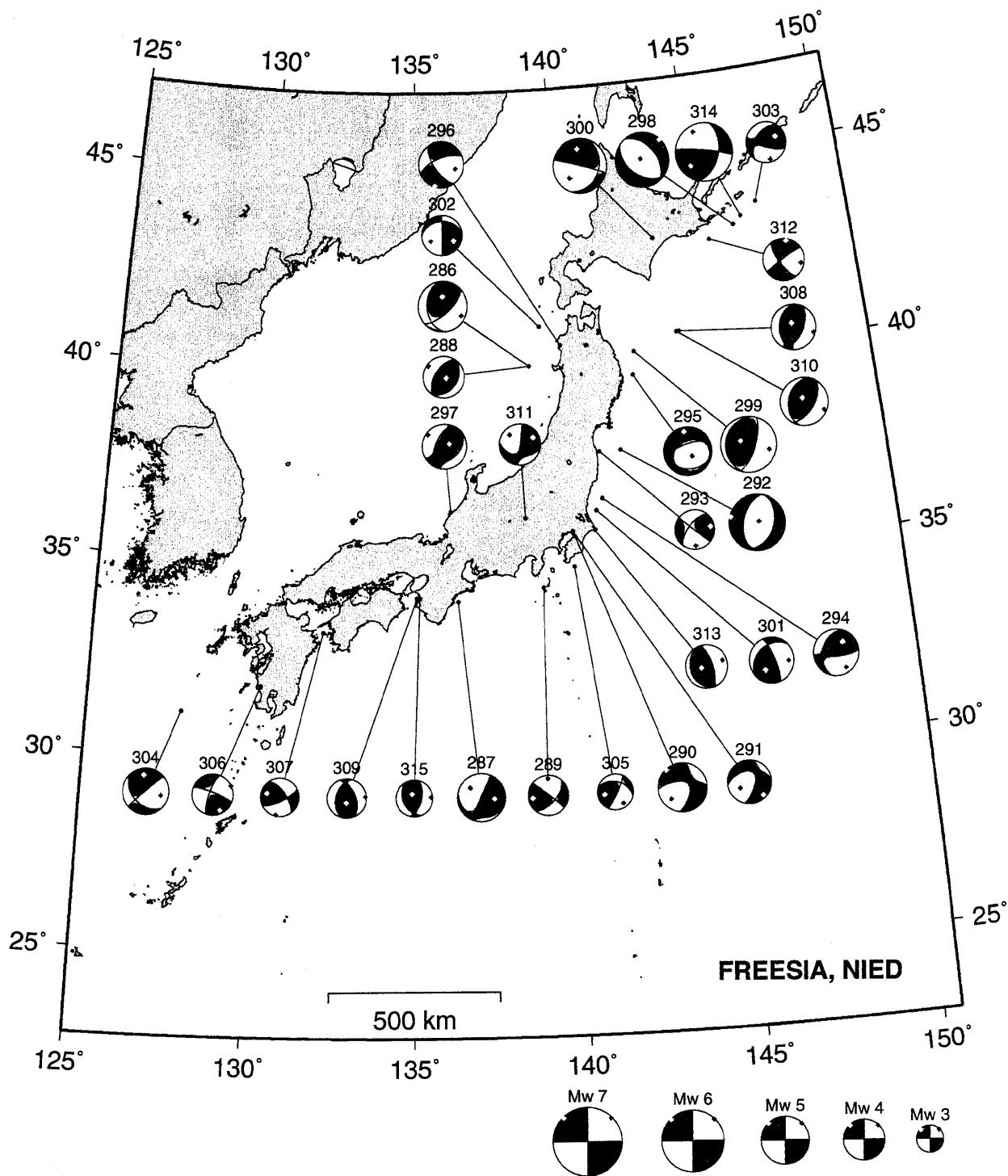


Fig. 2: Estimated moment tensors plotted with epicentral locations (continued).

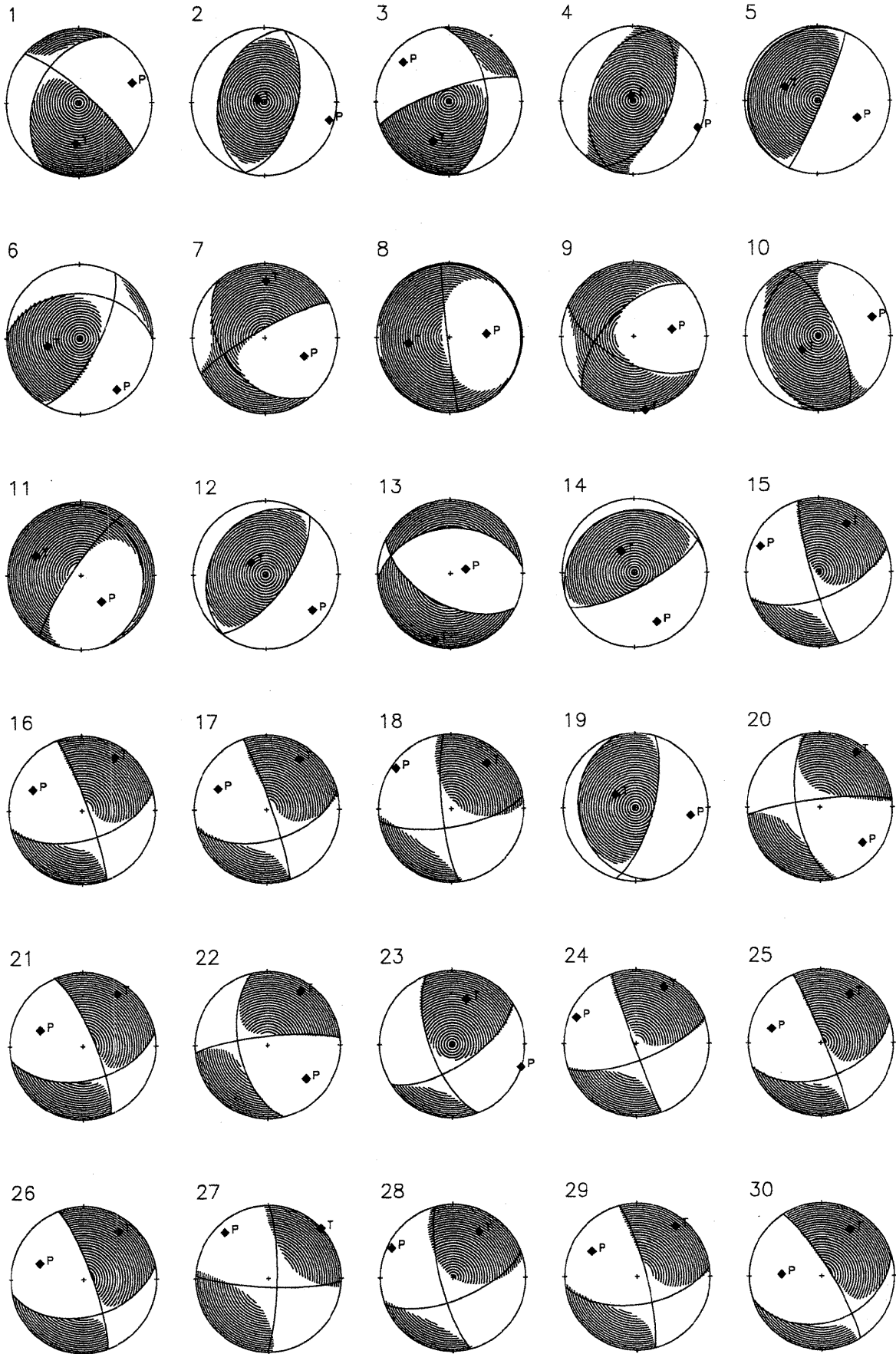


Fig. 3: Estimated moment tensors plotted in the lower hemisphere. P- and T- axes are also plotted.

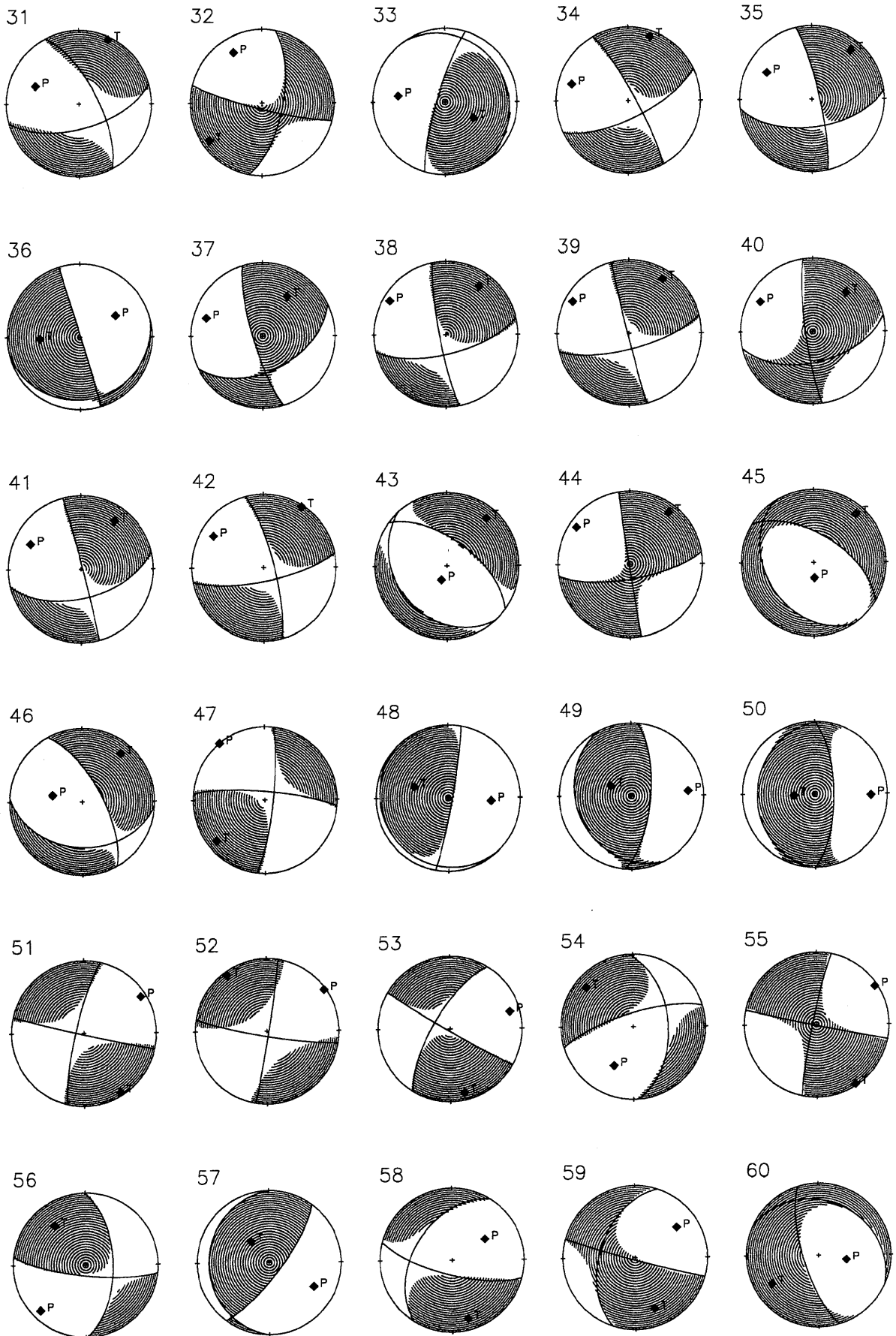


Fig. 3: Estimated moment tensors plotted to the lower hemisphere (continued).

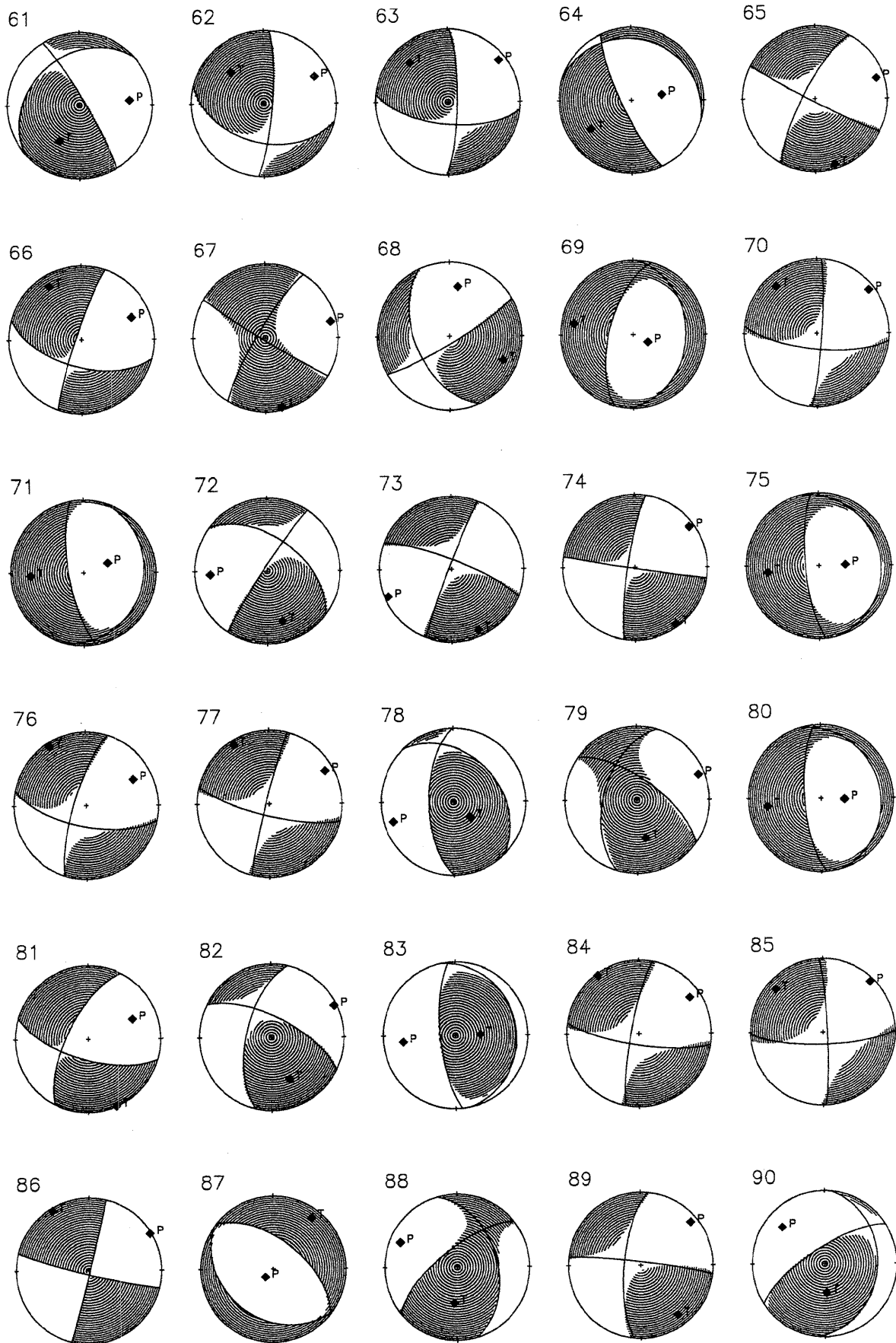


Fig. 3: Estimated moment tensors plotted to the lower hemisphere (continued).

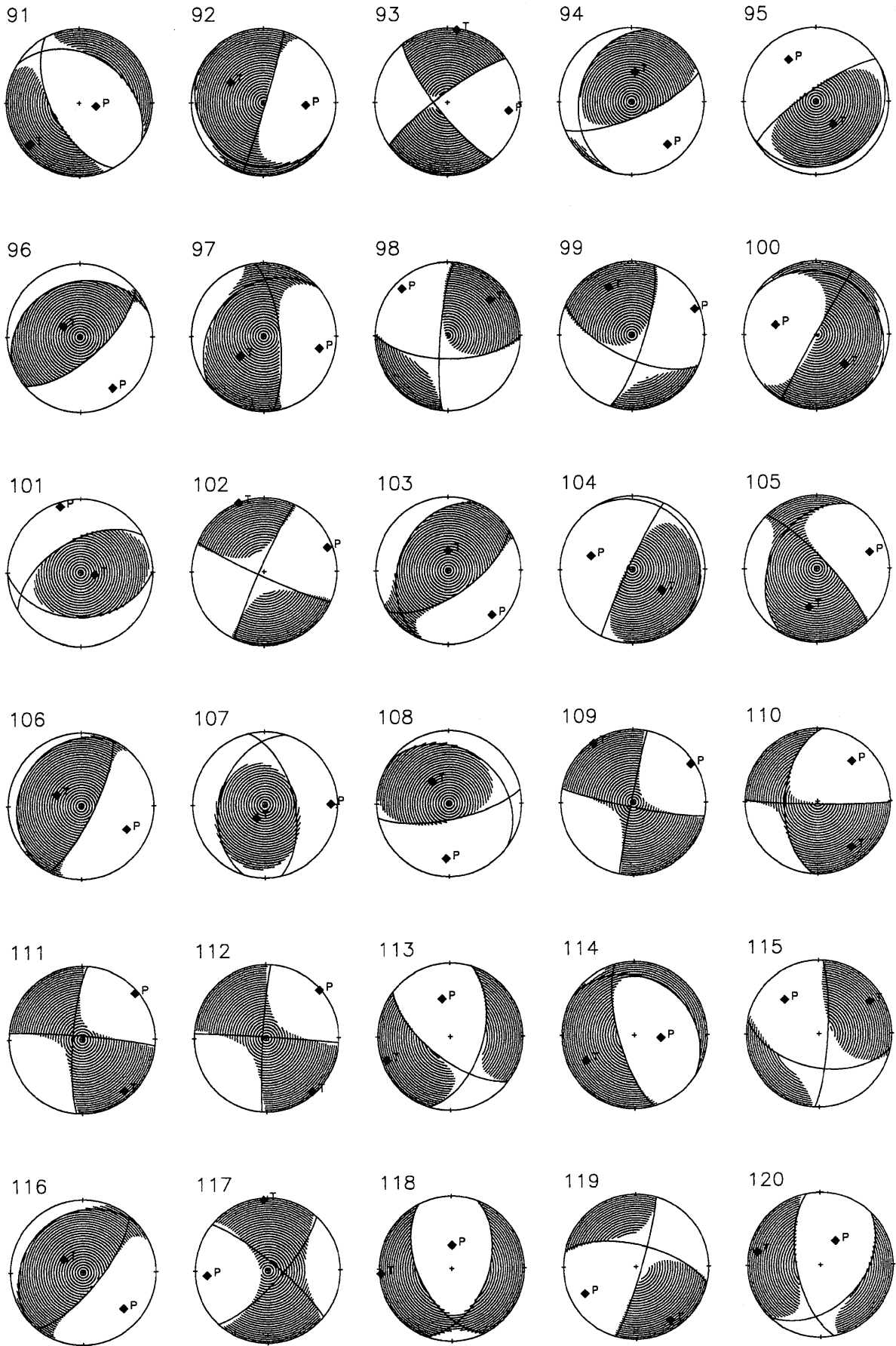


Fig. 3: Estimated moment tensors plotted to the lower hemisphere (continued).

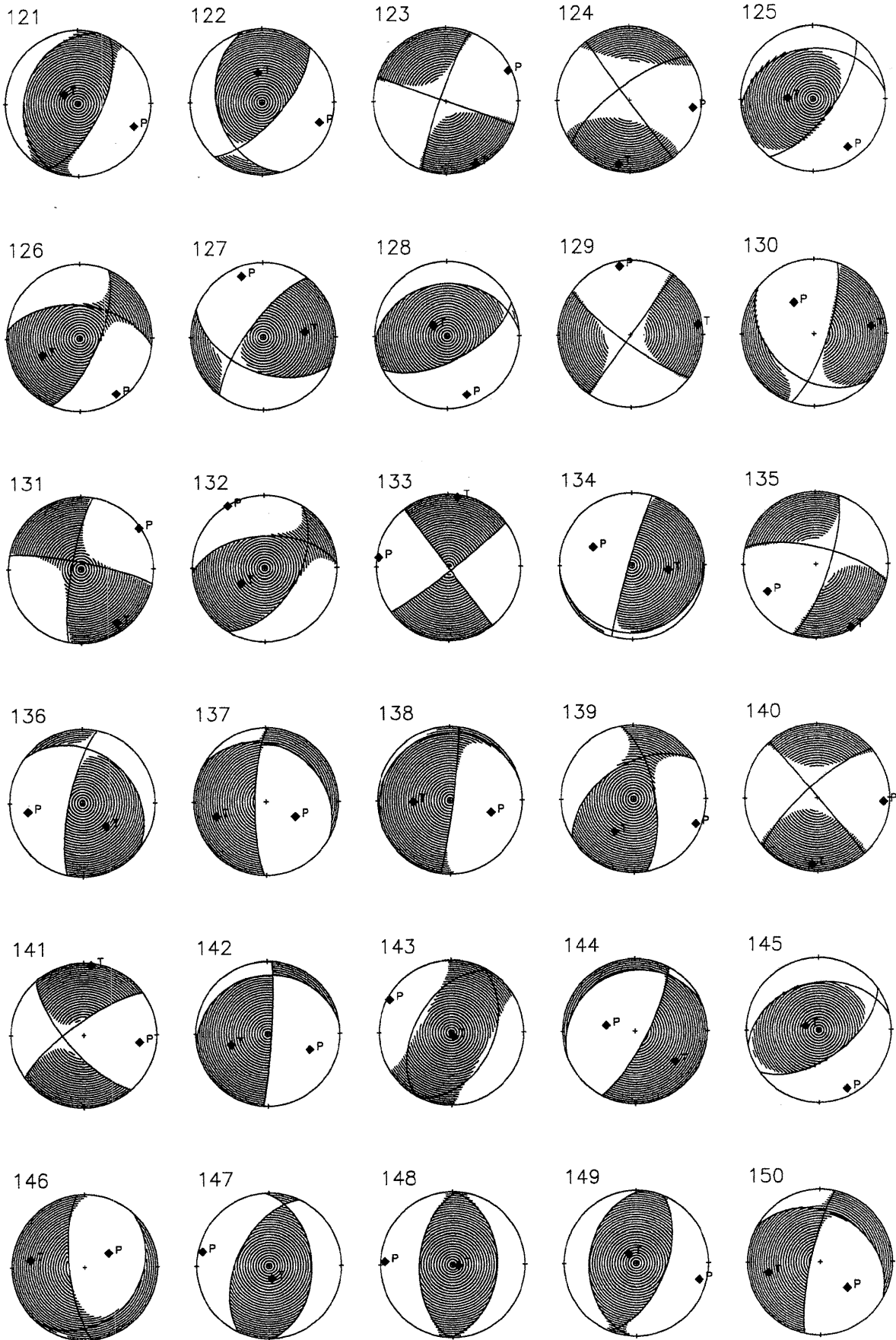


Fig. 3: Estimated moment tensors plotted to the lower hemisphere (continued).

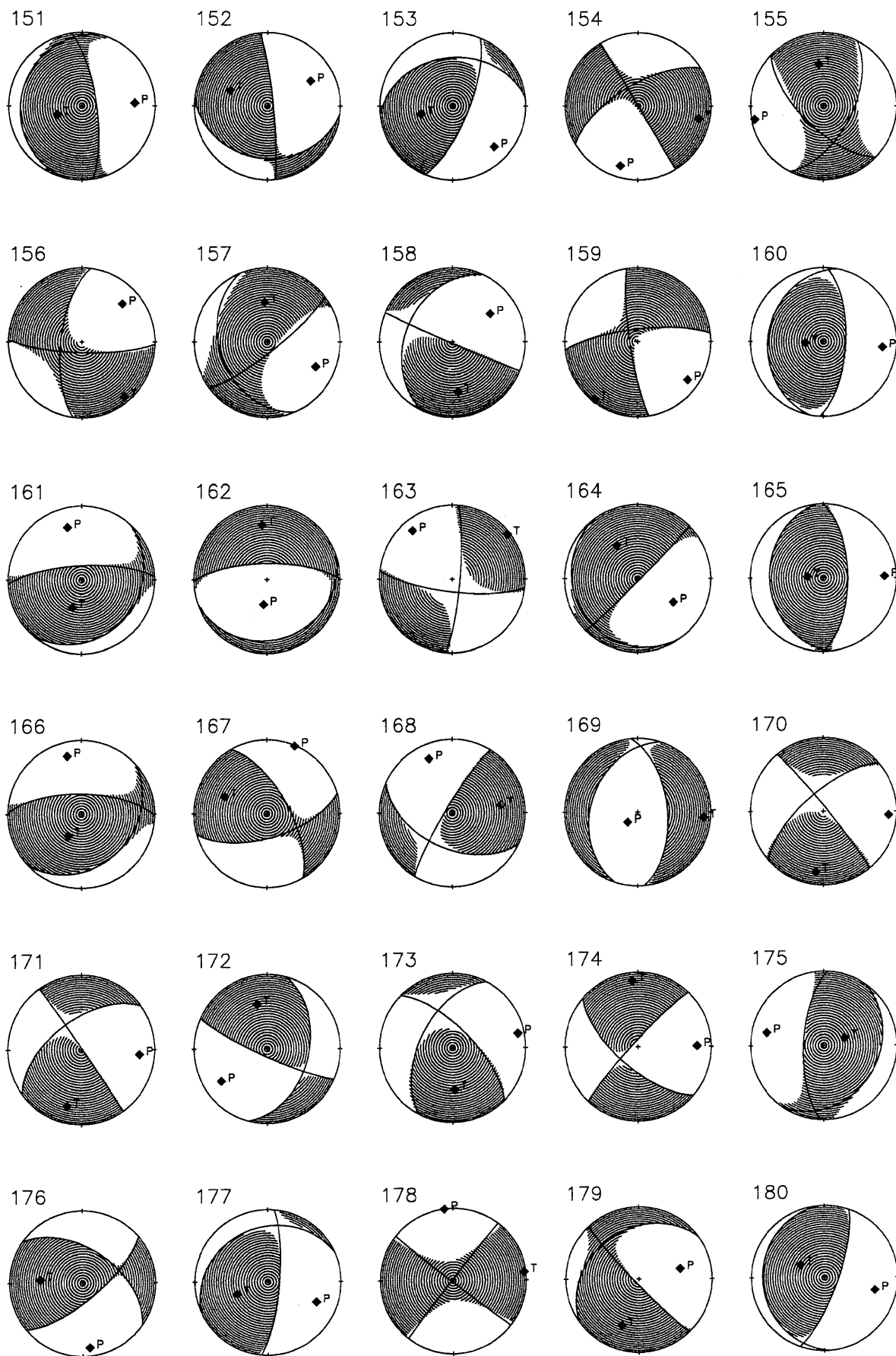


Fig. 3: Estimated moment tensors plotted to the lower hemisphere (continued).

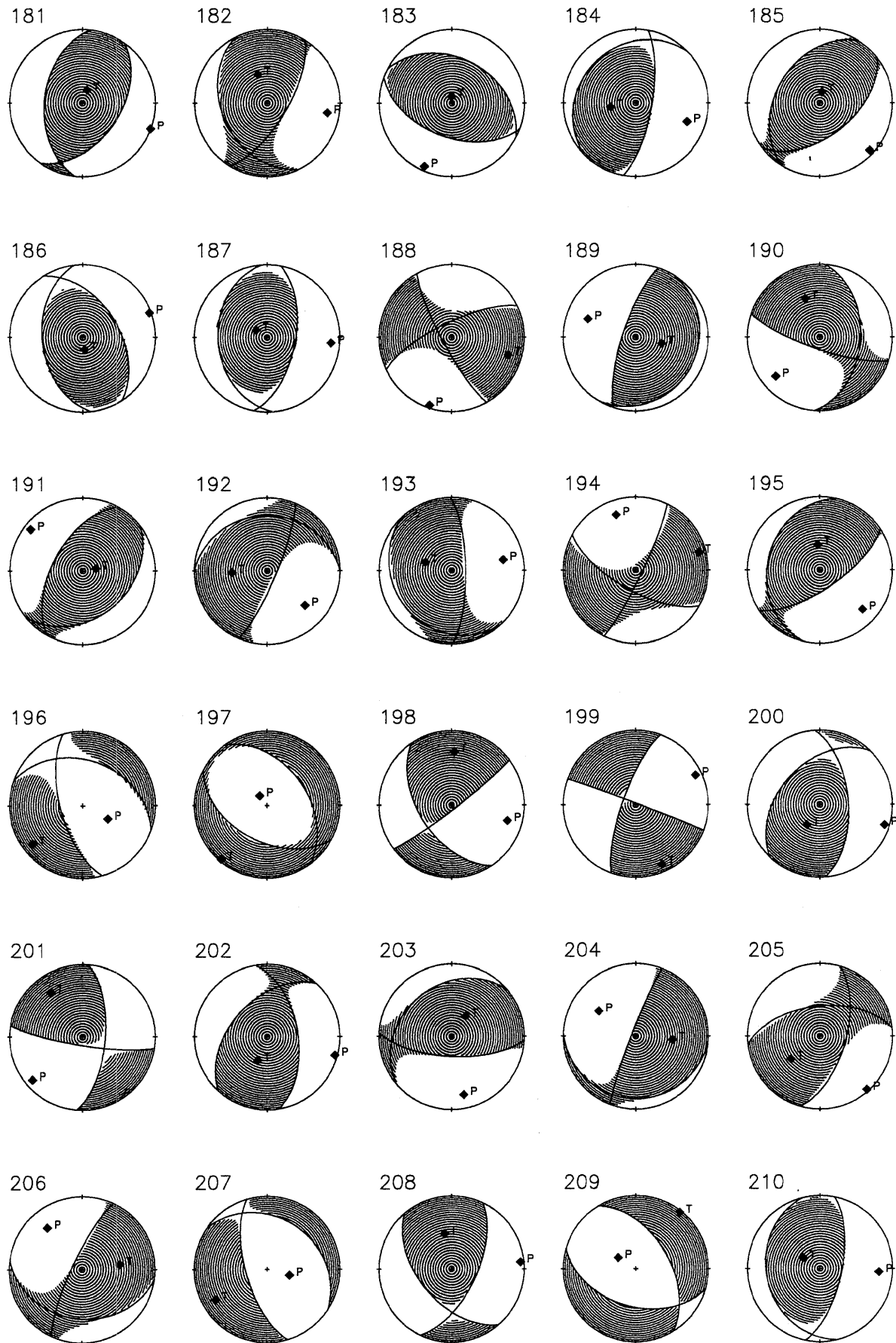


Fig. 3: Estimated moment tensors plotted to the lower hemisphere (continued).

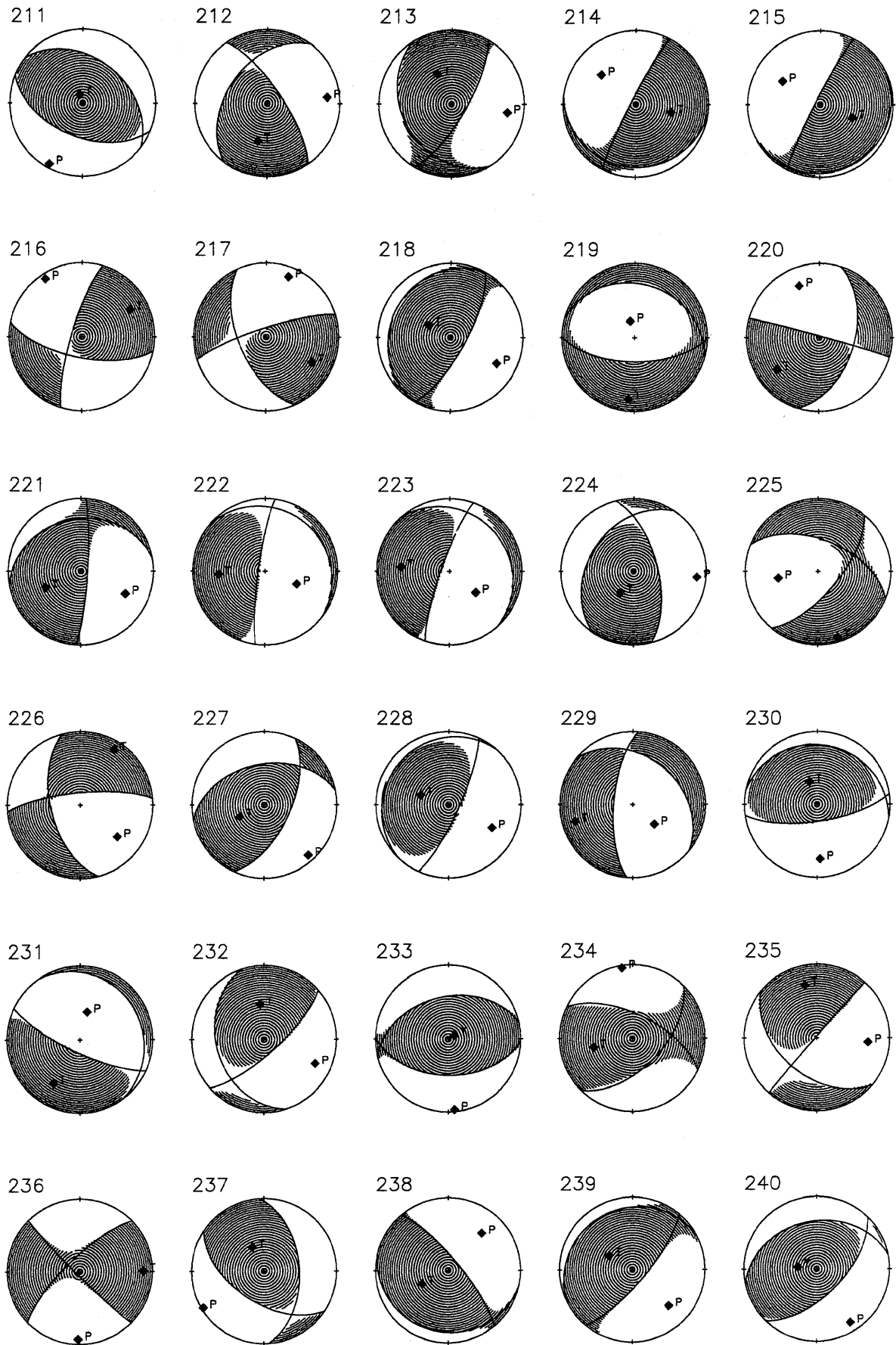


Fig. 3: Estimated moment tensors plotted to the lower hemisphere (continued).

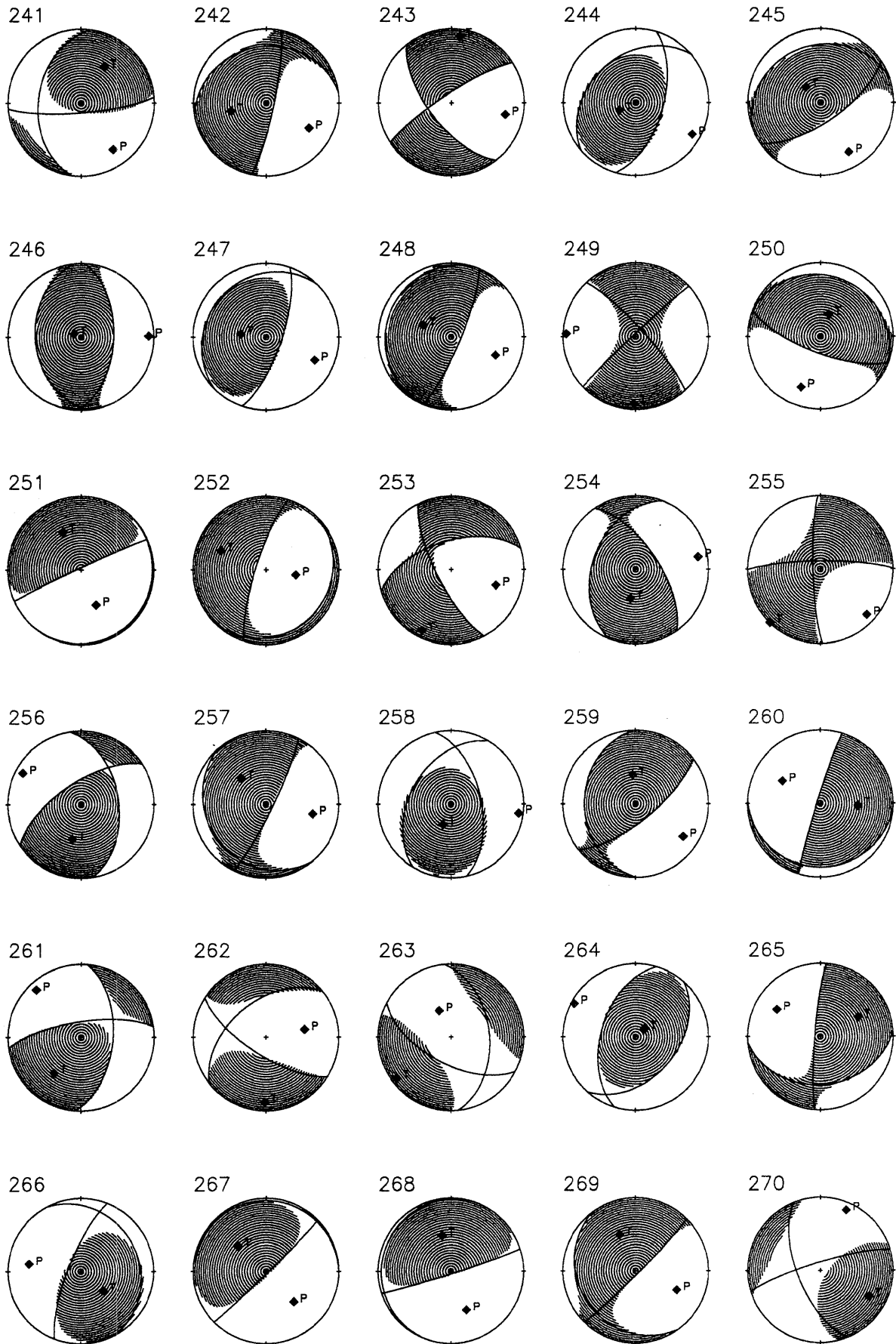


Fig. 3: Estimated moment tensors plotted to the lower hemisphere (continued).

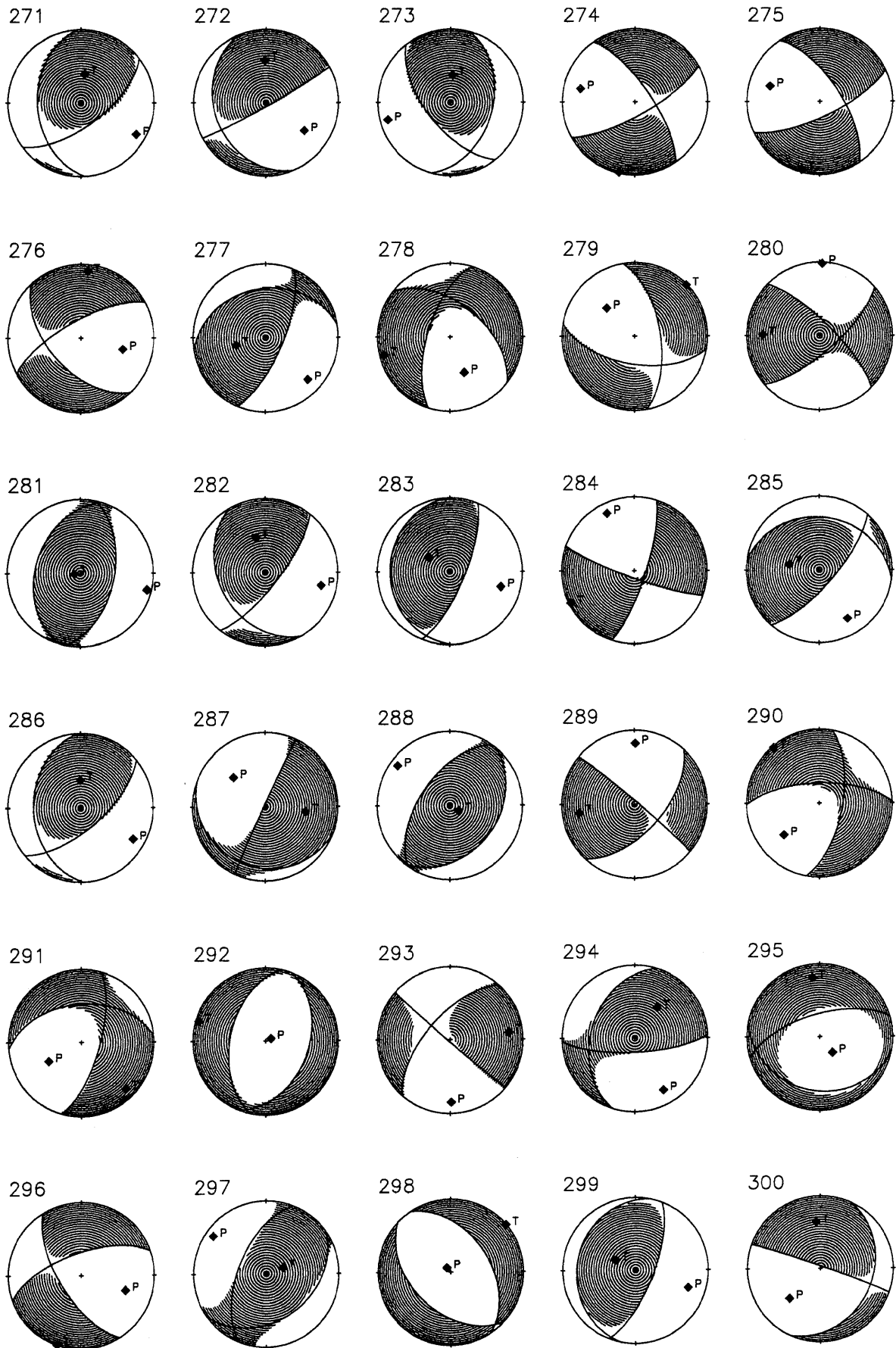


Fig. 3: Estimated moment tensors plotted to the lower hemisphere (continued).

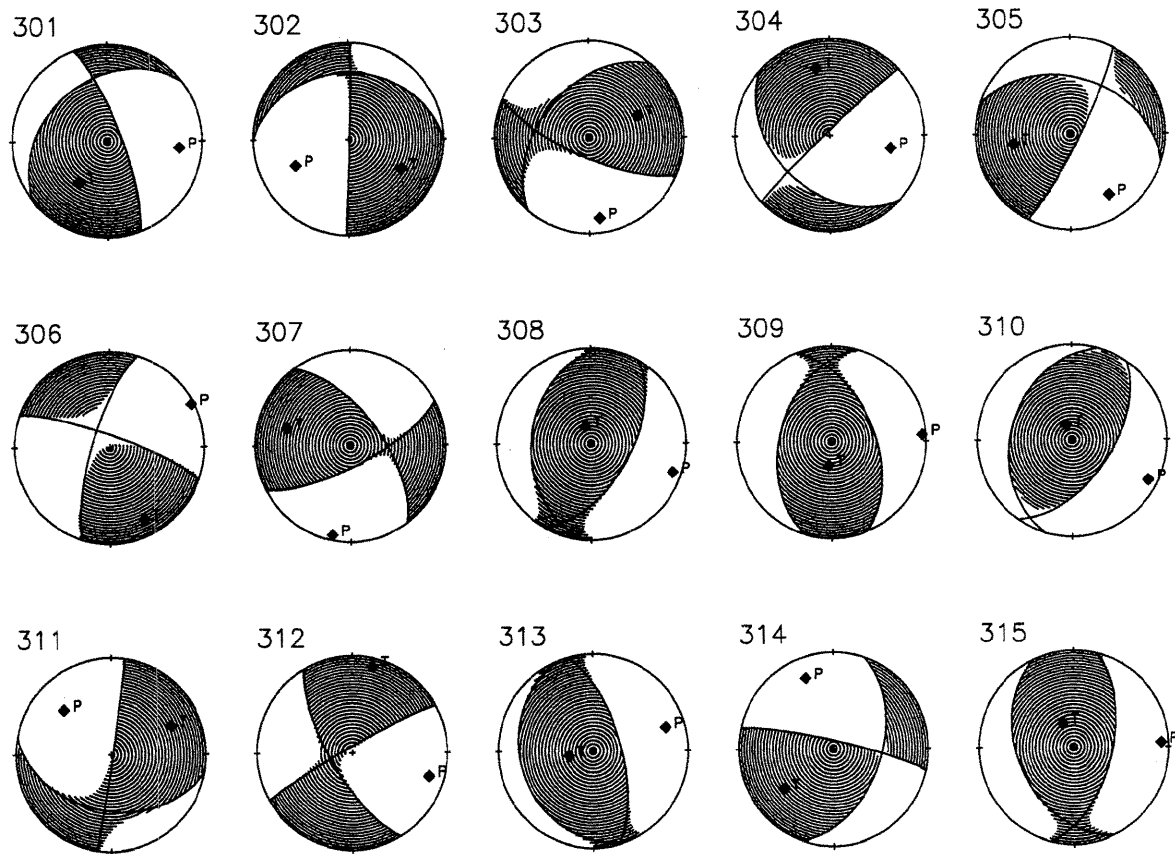


Fig. 3: Estimated moment tensors plotted to the lower hemisphere (continued).